13.19 Uranium Ore Deposits

K Kyser, Queen's University, Kingston, ON, Canada

13.19.1 Introduction

The discovery of uranium is attributed to Klaproth, a German chemist who, in 1789, precipitated a yellow compound by dissolving pitchblende in nitric acid, neutralizing it with sodium hydroxide, and heating it with charcoal to obtain a black powder that was uranium oxide. He named the newly discovered element after the planet Uranus. In 1841, Péligot, a French chemist working at the Baccarat crystal factory in Lorraine, isolated the first sample of uranium metal by heating uranium tetrachloride with potassium. Uranium was used during the nineteenth century to color pottery and glass until the discovery of radioactivity by Becquerel in 1896 (Becquerel, 1896), when he accidentally exposed a photographic plate to uranium. A team led by Enrico Fermi in 1934 observed that bombarding uranium with neutrons produces the emission of beta rays, and this led to the discovery of fission of uranium by the Fermi group on 2 December 1942 – the era of the power of the atom began.

Uranium is one of the most important energy-related materials, with current use almost entirely for generating electricity and a small proportion for producing medical isotopes. About 17% of the world's electricity is generated from reactors spread across 30 countries (EIA, 2007; OECD/NEA-IAEA, 2010), and energy generated from uranium has a minimal 'carbon footprint' (Pacala and Socolow, 2004). Although the effects of the natural disaster at Fukushima in 2011 on nuclear energy have caused many nations to reevaluate their nuclear energy programs, meeting the current, let alone the projected, needs of the uranium industry requires discovery of new

deposits and development of new technologies for both exploration and processing.

This chapter reviews current knowledge of major uranium deposits, along with some critical gaps in the understanding of them that also exist. It describes the most significant deposits, discusses their genesis, and places them in a regional context to aid future exploration. An additional focus is the uniqueness of uranium as a commodity and an ore-forming element. Uranium as a commodity differs from most others in that much of our knowledge has been eroded or has gone underground since the late 1970s when the perceived need for new deposits diminished. However, the demise of the former Soviet Union in 1991 made new data available, and the recent debate about uranium has stimulated the need to know more about how uranium behaves in the environment.

13.19.2 The Need for Uranium

The current major use of uranium is for the generation of electricity. The 438 nuclear power reactors and 270 research reactors require nearly 60 000 tU (155 million lbs U_3O_8) of uranium annually (OECD/NEA-IAEA, 2008, 2010). About 25% of these reactors are in North America and 37% are in Europe. Given all of the existing reactors, the 40 reactors currently under construction, and those anticipated, the need for uranium is anticipated to increase by about 30% to 82 000–100 000 tU (212–259 million lbs U_3O_8) by the year 2025 (EIA, 2007; OECD/NEA-IAEA, 2010).

The use of uranium as a fuel for nuclear reactors is not without its caveats. The operational, maintenance, and fuel costs for nuclear power are only half of that for fossil fuels, but nuclear power plants cost four times as much and require much longer times to build than plants that use fossil fuels (Ansolabehere et al., 2003). Securing licenses for nuclear power plants is an arduous and expensive task, as is getting acceptance by the local community. The lead time for building a nuclear power plant is lengthy, at least 10 years. The amount of spent fuel produced each year is about 12 000 t (Vance, 2008), but most of the potential energy in the fuel is not used. It contains fission products such as bioactive ^{131}I, ^{90}Sr, and ^{137}Cs with relatively short half-lives and many longer-lived, intensely radioactive isotopes such as ^{99}Tc, ^{140}Ce, and ^{239}Pu that render it dangerous.

The Uranium Group of the International Atomic Energy Agency (IAEA) and Organization for Economic Co-operation and Development (OECD)/Nuclear Energy Agency (NEA) classifies identified resources as those recoverable for <US $130 kg^{-1} U (US$50/pound U_3O_8), which is near the average 'price' of uranium for the past few years. Estimated global resources in 2009 were near 5.4 million tU at <US$130 kg^{-1}, with a distinct lack of geographic diversity because 73% of these resources are located in just five countries (Figure 1(a)) and the major ore deposit types in each is different. Over half of the uranium resources in the world are associated with sedimentary basins (Figure 1(b)). For example, in 2009, about 55% of uranium production was from deposits in basins. But there is geographic disparity in the distribution of uranium resources relative to the nations that rely heavily on nuclear power.

13.19.3 Geochemistry of Uranium

Uranium is an actinide element like thorium and has an atomic number of 92 and three main naturally occurring isotopes (^{234}U, ^{235}U, and ^{238}U), of which ^{238}U is the most abundant at 99.3%. Like Th, it is a radioactive element, and its most stable isotope, ^{238}U, has a very long half-life of 4.46×10^9 years. Uranium occurs in natural systems in three oxidation states, U^{4+}, U^{5+}, and U^{6+}, in contrast to Th, which occurs exclusively as Th^{4+}. In magmas, the highly charged U^{4+} ion behaves incompatibly, becoming concentrated in late-stage differentiates and in a variety of accessory minerals. Thus, granites and pegmatites produced from evolved magmas are richer in uranium than mafic igneous rocks (Table 1). Uranium is generally highest in felsic rocks and in peralkaline rocks over calc-alkalic and peraluminous equivalents, but secondary concentration of uranium may occur as a result of hydrothermal activity associated with the emplacement of any felsic volcanic and intrusives. In igneous rocks, uranium is associated with Th, Zr, Ti, Nb, and rare earth elements (REE), particularly for peralkaline rocks, but less so for metaluminous rocks and not at all for peraluminous rocks.

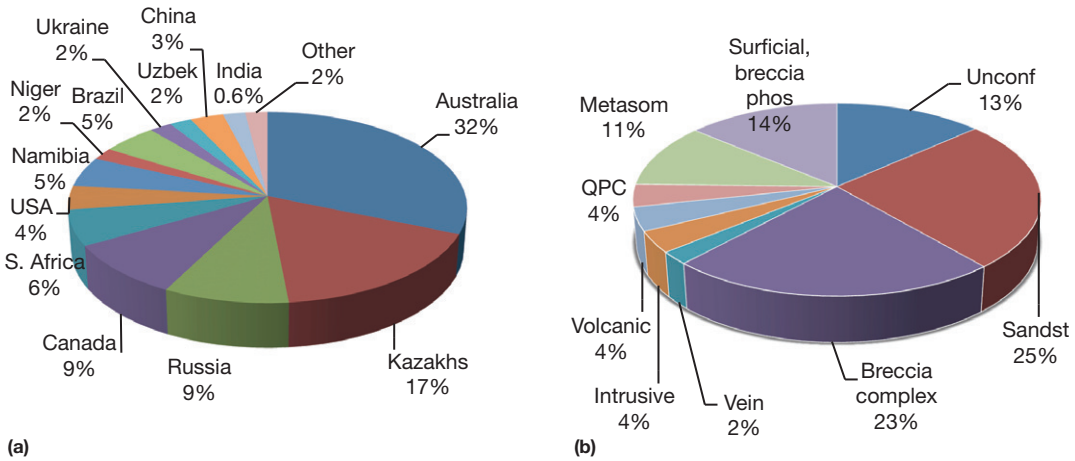

Figure 1 Percentage of global identified resources at <US$130 kg^{-1} (a) by country and (b) by deposit type in 2009. Data from OECD/NEA-IAEA (2010).

Table 1 Uranium concentrations in geologic materials

Reservoir	*ppm*
Average crust	1.7
Oceanic crust	0.5
Upper continental crust	2.7
Peridotites	0.003–0.05
Eclogites	0.013–0.8
Average basalt	0.3
Mid-ocean ridge basalt (MORB)	0.07–0.1
Continental andesites	0.5–1.0
Island arc andesites	0.2–0.4
Average granodiorite	2.0
Average granite	3.8
Nepheline syenites	200–600
Alkali granites	20–200
Common shale	3.7
Black shale	3–1250
Sandstones	0.45–3.2
Average carbonate rock	2.2
Marine phosphates	50–300
Evaporites	0.01–0.43
Seawater	0.003

In other lithologic environments, uranium is most closely associated with redox active elements such as Mo, V, Se, As, and Cu. Levels of uranium in sedimentary rocks are closely related to their redox conditions, with the highest concentrations found in organic-rich facies associated with anoxic environments and phosphatic sediments (**Table 1**).

Uranium occurs in rocks as its own minerals, as a substitute element in rock-forming and accessory minerals, in exchangeable positions in zeolites and clays, adsorbed on crystal faces, and dissolved in intergranular fluids and fluid inclusions. The mineralogy of uranium is controlled by its high charge density, and the two principal minerals are uraninite (written as UO_2 but chemically UO_{2+x}; Janeczek and Ewing, 1992) and coffinite ($USiO_4$). Pitchblende is a general term given to the fine-grained, massive colloform variety of uraninite. Additional common minerals include brannerite $(U,Ca,Ce)(Ti,Fe)_2O_6$ and uranothorite $(Th,U)SiO_4$. Uranium also occurs as highly colored hexavalent U minerals as primary ore minerals, such as carnotite $K_2(UO_2)_2(VO_4)_2{\cdot}3H_2O$, tyuyamunite $Ca(UO_2)_2(VO_4)_2{\cdot}3H_2O$, or after the alteration of uraninite such as autunite $Ca(UO_2)_2(PO_4)_2{\cdot}10H_2O$ or uranophane $Ca(UO_2)_2SiO_3(OH)_2{\cdot}5H_2O$ (Burns, 1999; Finch and Murakami, 1999). In reducing environments, uranium occurs as uraninite, coffinite, and phosphates, and in organic compounds, as thucholite. Approximately 5% of all known minerals contain uranium as an essential structural constituent (Burns, 1999).

The degree of substitution of uranium into accessory minerals is controlled by its effective ionic radius in the octahedral coordination of 1.00 Å for U^{4+}. Complete substitution occurs with Th^{4+}, limited substitution occurs for Ca^{2+} in rock-forming minerals and for Zr^{4+}, Nb^{5+}, and Ta^{5+} in accessory minerals, and extensive substitution of uranous ion occurs for REE in rare earth fluorocarbonates and phosphates.

The aqueous geochemistry of uranium is unusual in that uranium is generally more soluble in oxidizing, alkaline water than in reducing, acidic water due primarily to the tendency of U^{6+} to form strong complexes in oxidizing fluids, regardless of the temperature (**Figure 2**). Uranium is readily soluble in the strongly acid, oxidizing water often associated with acid mine drainage because the hydrated cation UO_2^{2+} and fluoro complexes of uranium are stable below pH 4 (**Figure 2**). In oxidized fluids between pH 4 and 7.5, uranyl phosphate complexes are the important species and at higher pH, uranyl carbonate complexes are dominant. In groundwater with normal sulfate concentrations of 100 ppm, uranyl sulfate complexes can be a significant species at pH < 7. However, the uranyl phosphate complex is so stable that for oxidizing groundwaters with typical concentrations of 0.1 ppm PO_4, this complex predominates over all others from pH 4 to 10 (**Figure 2**). In reduced groundwaters, only fluoride complexes of U^{4+} are significant and only at very low pH (Langmuir, 1978).

The extrapolated solubility of UO_2 in brines appears to be independent of pH in the range 4 to10 and has minimal temperature dependence from 100 to 300 °C (Parks and Pohl, 1988). Uranyl carbonate complexes are dominant under relatively oxidizing and near-neutral pH conditions, and chloride and sulfate complexes are dominant in oxidizing fluids under acidic conditions at temperatures up to 200 °C. Phosphate complexes remain dominant at neutral pH despite the emergence of important hydroxyl complexes at high pH (**Figure 2**).

Even moderate temperature changes in the fluid will not result in precipitation of uraninite, and only an increase in pH or a decrease in the activity of oxygen facilitates the precipitation of uraninite (Romberger et al., 1984). At 200 °C and high oxygen activities, hematite, a mineral commonly associated with hydrothermal uranium deposits, would also form, whereas at low activities, pyrite would be coeval with uraninite. In addition, U^{6+} reduction by reaction with Fe^{2+} or reduced carbon species (graphite does not seem to be reactive below 400 °C and must first be converted to hydrocarbon compounds) is the most likely mechanism by which uraninite precipitates from fluids.

Experiments on the solubility of large, highly charged ions like uranium in silicate melts indicate that solubility increases with the degree of depolymerization of the melts (Farges et al., 1992), which depends grossly on the molar excess of Na + K + Ca relative to Al and the temperature. Increasing either one results in breaking of the Si–Al tetrahedron chains in the silicate melt, thereby enhancing depolymerization and the solubility of large, highly charged ions. Uranium solubility in melts increases significantly when (Na + K)/Al ratios increase from 0.7 (peraluminous) to 1.6 (peralkaline) (Peiffert et al., 1996). Increasing the oxygen fugacity or the presence of carbon dioxide or chlorine in an aqueous fluid in equilibrium with the silicate melt has a minimal effect on the solubility of uranium in the melt. However, fluorine reacts with Al to form AlF_6^{3-}, thereby depolymerizing the tetrahedral aluminosilicate framework (Manning, 1981; Schaller et al., 1992) and enhancing the uranium solubility in the melt by 10–100 times.

The solubility of uranium in an aqueous fluid in equilibrium with a silicate melt increases with increasing oxygen fugacity and chloride concentration (Peiffert et al., 1994, 1996). Under oxidizing conditions, high solubilities of uranium in the fluid of up to 170 ppm result from the formation of U^{6+} chloride or hydroxyl–chloride complexes. Chloride in the fluids is much more effective than carbonate or fluoride in

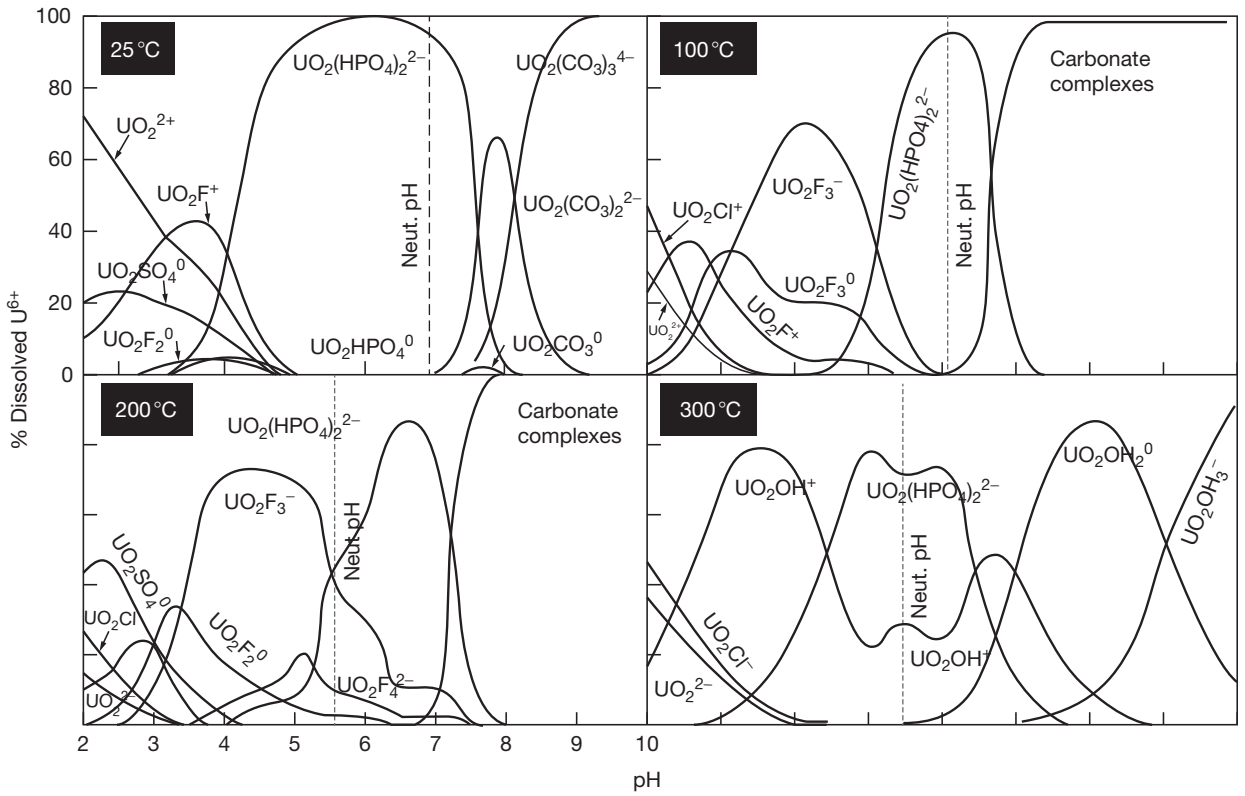

Figure 2 Relative concentration of uranyl complexes versus pH at 25 °C for a fluid with $\Sigma U^{6+} = 10^{-8}$ m, $\Sigma F = 0.3$ ppm, $\Sigma Cl = 10$ ppm, $\Sigma SO_4 = 100$ ppm, $\Sigma PO_4 = 0.1$ ppm, $\Sigma SiO_2 = 30$ ppm, and $P_{CO_2} = 10^{-2.5}$ atm; at 100 °C for a fluid with $\Sigma F = 10$ ppm, NaCl = 1 m, $\Sigma SO_4 = 1000$ ppm, $\Sigma PO_4 = 0.1$ ppm, and $P_{CO_2} = 1$ atm; at 200 °C for a fluid with $\Sigma F = 100$ ppm, NaCl = 1 m, $\Sigma SO_4 = 1000$ ppm, $\Sigma PO_4 = 1$ ppm, and $P_{CO_2} = 1$ atm; and at 300 °C for a fluid with $\Sigma F = 10$ ppm, NaCl = 1 m, $\Sigma SO_4 = 1000$ ppm, $\Sigma PO_4 = 10$ ppm, and $P_{CO_2} = 10$ atm. Reproduced from Kyser K and Cuney M (2009) Unconformity-related uranium deposits. In: Cuney M and Kyser K (eds.) *Recent and Not-So-Recent Developments in Uranium Deposits and Implications for Exploration*, *Mineralogical Association of Canada Short Course Series*, vol. 39, pp. 161–220. Quebec: Mineralogical Association of Canada.

increasing the solubility of uranium in the fluid, except in reducing, acidic fluids where fluoride enhances the solubility of uranium in the fluid.

13.19.4 Uranium Deposits Through Time

The ultimate origin of all uranium is from the mantle, but the most important concentrations involve relatively low-temperature processes, transport of oxidized uranium in fluids, and reduction reactions or changes in solubility. As a consequence, important deposits of uranium did not occur until the oxygen content of the atmosphere was high enough in surficial fluids to mobilize uranium as U^{6+} and the biosphere had evolved to become a significant quantity of reductant.

During the Archean, uranium could not be concentrated in significant quantities until elemental cycling from tectonics allowed the production of fractionated peralkaline melts (Cuney, 2010), which did not occur until after 3200 Ma. The Archean and early Paleoproterozoic saw uranium deposited in placer deposits, but these become rare in the Paleoproterozoic because of increases in the oxygen levels in the atmosphere after 2200 Ma.

The Paleoproterozoic era (2500–1600 Ma) is a period of Earth history characterized by substantial orogens associated with the assemblage of the megacontinents of Arctica (Canada, Siberia, and parts of Greenland) and Atlantica (Africa and South America). Growth of Arctica occurred during the Paleoproterozoic and through the beginning of the Mesoproterozoic with the accretion of Baltica, North America, and East Antarctica into the larger continent of Nena (Cawood et al., 2007; Rogers and Santosh, 2002; Zhao et al., 2002). These orogens gave rise to enhanced uranium concentrations in high-heat-flow granites, whose eventual erosion would supply U-rich minerals to sedimentary basins that would form in response to down-warping due to plate loading and rifting. Metamorphism of large areas of the crust also occurred, resulting in significant high-temperature sodic fluids that carried uranium and produced metasomatic-type deposits (Cuney, 2010).

The end of the Paleoproterozoic and beginning of the Mesoproterozoic is marked by the general termination of orogens and a period of continental readjustment and relative tectonic quiet for about 500 My, during which several large intracratonic basins formed and evolved. During this period, the basins and the fluids they contained would be affected by far-field tectonic events associated with the readjustment, which resulted in changing the hydraulic gradients within the basins and caused basinal brines to flow. Atlantica and other continental blocks would be accreted to Nena during the Grenville event at *c*.1.0 Ga to form the supercontinent Rodinia. Near the termination of the Proterozoic, the Earth becomes agitated once again as the megacontinent Rodinia is

tectonically dissected into several fragments, mainly along suture zones formed previously (Rogers and Santosh, 2002). As a consequence, many of the basins remained intact and would remain so unless deformed by later tectonic events. Formation of economic uranium deposits shifted to the subsurface of intracratonic and rift basins as oxidized basinal brines mobilized and transported U^{6+} that could be concentrated by effective reductants (Hazen et al., 2008, 2009).

When land plants evolved in the early Phanerozoic, the Earth witnessed for the first time large deposits of terrestrial organic matter along with stabilized soils that promoted cohesive riverbanks and meandering stream systems. As a result, mud is found in many Phanerozoic sedimentary successions deposited in fluvial environments, and these serve to confine aquifers for later focused fluid events related to the deposits that formed in sandstone aquifers having abundant terrestrial organic matter or their diagenetic products (Hiatt et al., 2007).

13.19.5 Deposit Types

There are many different ways of classifying uranium deposits depending on the tendency of the classifier to put deposits into more generic classes or divide deposits according to their style of occurrence. No classification is perfect, as many types of deposits fall between the boundaries or are composites of deposit types. The most widely used classification by most uranium mining companies and researchers is that from the OECD/IAEA (OECD, 2001; OECD/NEA-IAEA, 2008, 2010), which divides deposits into 15 categories based on the geologic environment and character of the uranium mineralization as shown in **Figure 3**. One of the problems with subdividing deposits is that a genetic connotation can be implied, but one of the advantages is that the model of formation or location that is implied can be used to refine exploration strategies.

Twelve deposit types are described here, but they encompass nearly all those defined by the OECD/IAEA. Grade and tonnages indicate that, except for iron oxide–copper–gold–ore (IOCG) deposits, namely, Olympic Dam, unconformity-related deposits have the highest grade and tonnage (**Figure 4**). As a group, deposits associated with sedimentary basins are the most significant (**Figure 1(b)**).

13.19.5.1 Unconformity-Related Deposits

Unconformity-related deposits occur close to major unconformities between Archean–Paleoproterozoic metasedimentary rocks and overlying Paleo–Mesoproterozoic sandstone units in large marginal or intracratonic basins (**Figure 5**). The deposits occur within the basement or sandstone, but within a few hundred meters of the unconformity. The deposits are hosted by faults and are commonly associated with brecciation. The formation of these deposits is related to a reduction front near the unconformity between Paleoproterozoic sandstones and underlying metamorphosed basement lithologies. They involve formation from basinal brines at 200–250 °C, so far are restricted to the Proterozoic, and formed within 150 My after the basins formed (Kyser and Cuney, 2009). Unconformity-related deposits include some of the largest and richest uranium deposits (**Figure 4**).

Current models for the formation of the deposits can be divided into two general end-members. One involves the basement as the source of the uranium and the basins as the source of the fluids (Cuney et al., 2003), and the other involves the overlying basin as a source for both the uranium and fluid (Hoeve and Sibbald, 1978; Kyser et al., 2000). The basement model sources uranium from the breakdown of monazite along fault zones as basinal brines interact with the basement. In the basin model, uranium is precipitated when the oxidized

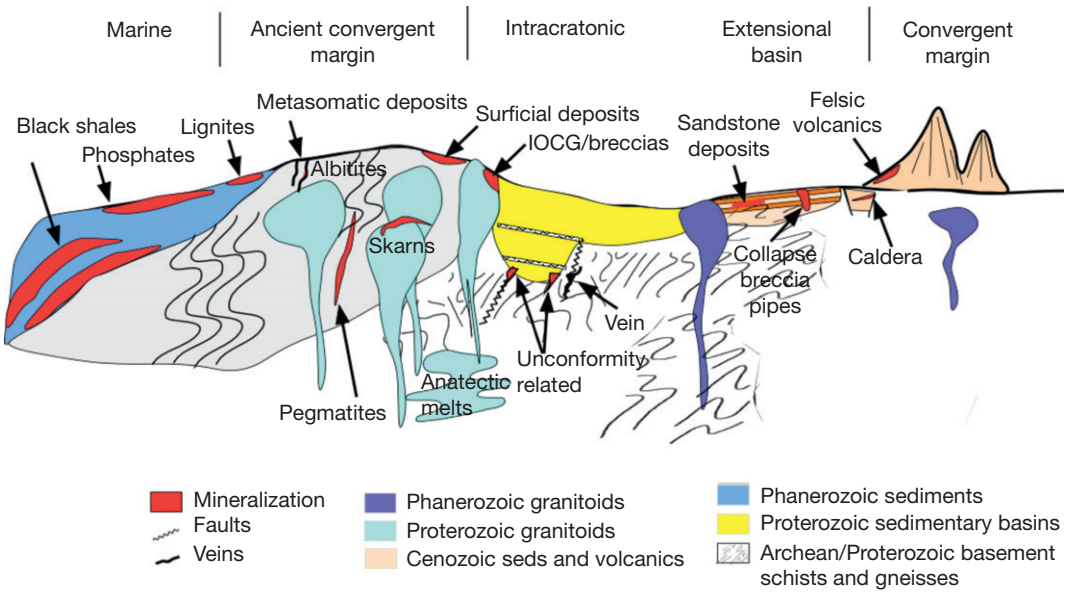

Figure 3 Schematic representation of the location of various types of uranium deposits. Reproduced from Kyser K and Cuney M (2009) Unconformity-related uranium deposits. In: Cuney M and Kyser K (eds.) *Recent and Not-So-Recent Developments in Uranium Deposits and Implications for Exploration*, *Mineralogical Association of Canada Short Course Series*, vol. 39, pp. 161–220. Quebec: Mineralogical Association of Canada.

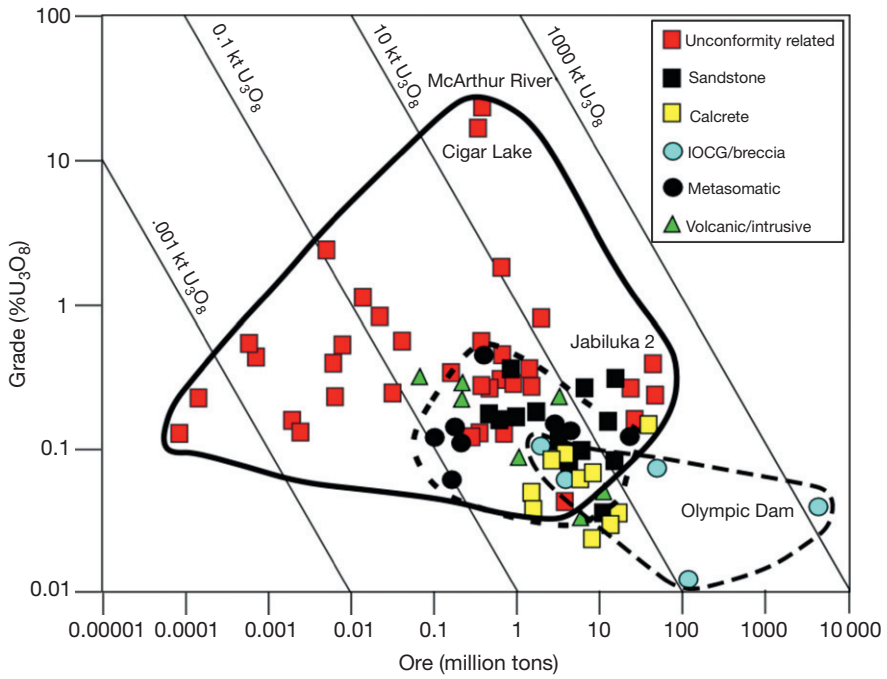

Figure 4 Grade versus tonnage for the major types of uranium ore deposits. Unconformity-related deposits, encompassed by the solid line, have the highest grade and have large reserves. Particularly high grades and reserves characterize the deposits at Cigar Lake and McArthur River in the Athabasca Basin and the Jabiluka 2 deposit in Australia. Volcanic/intrusive, metasomatic, sandstone, and calcrete uranium deposits, indicated by the group surrounded by the short dashed line, have much lower grades and are smaller, as are iron oxide–copper–gold–ore (IOCG)/breccia-related deposits, shown by group indicated by the long dashed line, except for Olympic Dam where uranium is a by-product.

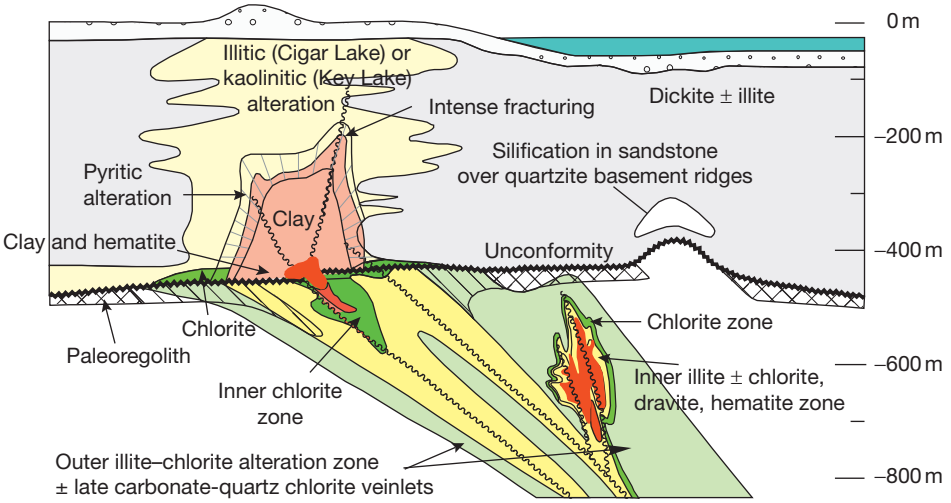

Figure 5 General components and geology of Proterozoic unconformity-related uranium deposits showing basement- and basin-hosted types.

basinal brine carrying uranium interacts with a reduced basement lithology (Hoeve and Sibbald, 1978), encounters reductants in the basin such as volcanic units (Holk et al., 2003), or mixes with basement-derived, reduced fluids (Fayek and Kyser, 1997). The source of the uranium in the basin model is from the breakdown of uranium-bearing detrital phases by basinal fluids in deep-basin paleoaquifers.

The most significant deposits are hosted by the Paleoproterozoic Athabasca Basin in Canada and the Kombolgie Basin in Australia, supplying 30% of the global uranium market (Sibbald and Quirt, 1987; Thomas et al., 2000). Other Proterozoic unconformity-related deposits not yet exploited but under study include the Kiggavik trend deposits proximal to the Thelon Basin in Canada, the Karku deposit in the Pasha–Ladoga Basin in Russia, and the Otish Basin in Quebec.

13.19.5.1.1 The Athabasca Basin

The Athabasca Basin hosts the largest and highest-grade uranium deposits globally (Figure 4) and is currently the sole source of uranium from Canada. The average grade for all mined unconformity deposits in the Athabasca Basin is 2% U (Gandhi, 2007), five times the average grade of 0.4% for the Australian

unconformity-related deposits, and it is still considered one of the most prospective areas for uranium exploration. Because of the wealth of deposits in the Athabasca Basin, it is the standard to which all basins are compared for prospectivity.

The Athabasca Basin is located in the Western Churchill province between the eroded remnants of two major orogenic belts, the 1.8 Ga Trans-Hudson orogen to the southeast and the 1.9 Ga Taltson Magmatic Zone to the northwest, which accommodated the convergence of the Slave and Superior provinces (e.g., Hoffman, 1988) and formed the Rae and Hearne provinces (Figure 6). In the eastern part of the Athabasca Basin, the great majority of mines and prospects are located where the Athabasca Group unconformably overlies the western Wollaston basement domains, with many deposits located around graphitic metapelites. Uranium mineralization in the western Athabasca Basin is also associated with graphitic shear zones in the underlying basement in the Taltson Magmatic Zone (Card et al., 2007).

There is a well-developed paleoregolith on the crystalline basement rocks underlying the Athabasca Group sediments that extends to a depth of several meters, signifying a period of erosion and weathering prior to the deposition of the

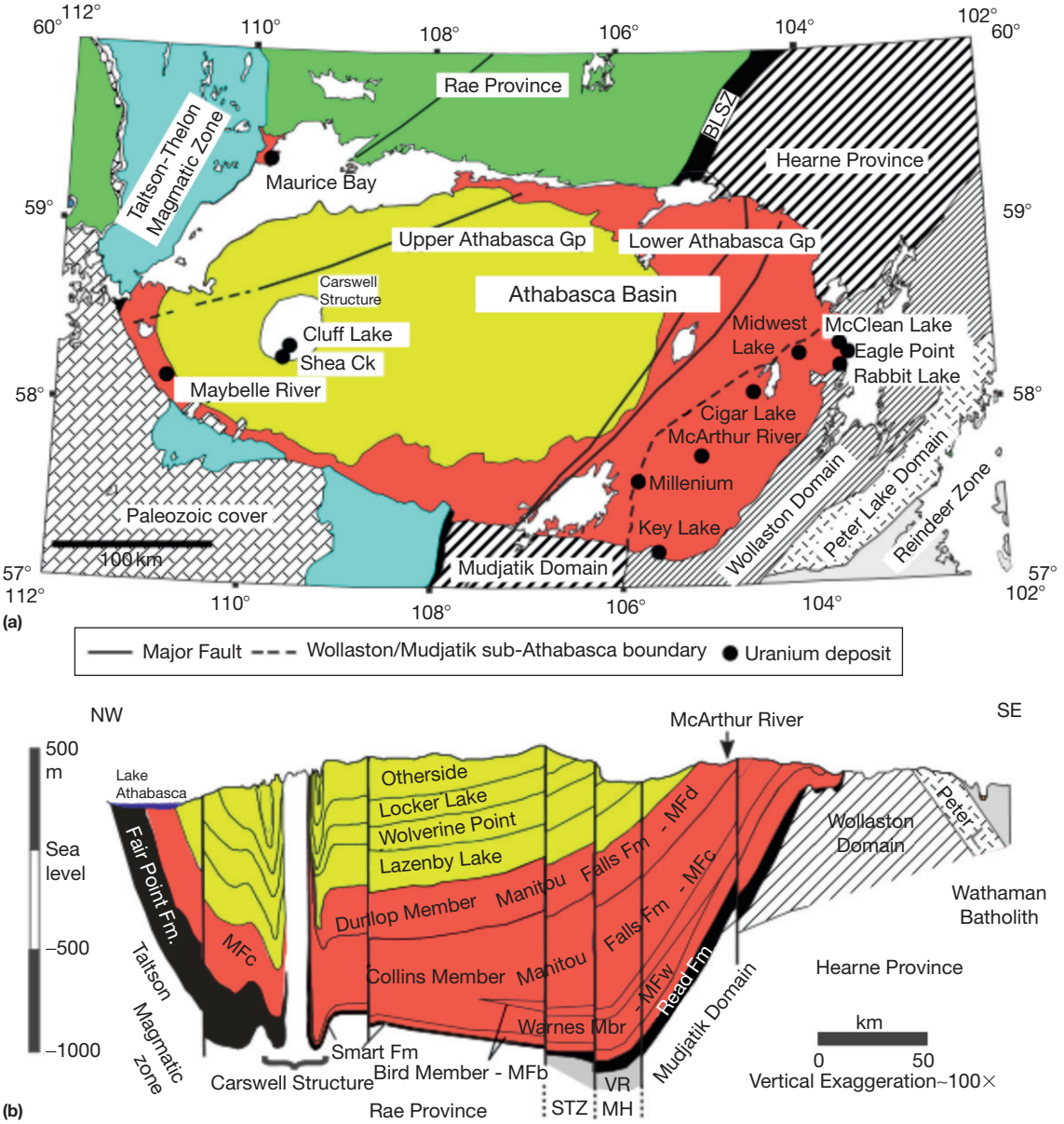

Figure 6 (a) General geology of the Athabasca Basin showing various domains that make up the basement units and location of various unconformity-related deposits. (b) Generalized cross section from NW to SE of the Athabasca Basin showing the stratigraphic units and their distribution. Formation and member names from Jefferson CW, Thomas DJ, Gandhi SS, et al. (2007) Unconformity-associated uranium deposits of the Athabasca Basin, Saskatchewan and Alberta. In: Jefferson CW and Delaney G (eds.) *EXTECH IV: Geology and Uranium EXploration TECHnology of the Proterozoic Athabasca Basin, Saskatchewan and Alberta, Geological Survey of Canada Bulletin 588*, pp. 23–68. Ottawa, ON: Geological Survey of Canada. Reproduced with permission from the Society of Economic Geologists.

Athabasca Group. This regolith is unconformably overlain by the basal portion of the Manitou Falls Formation, which is most associated with the deposits. The basal units are composed of conglomerates with attributes that reflect deposition in high-energy braided streams or alluvial fan settings. The middle interval represents deposition in more distal braided stream environments and had lower hydraulic conductivities. The sandstones that make up the upper third to half of the Manitou Falls Formation consist of medium-grained sandstone with mud rip-up clasts, consistent with deposition in lower energy, distal braided stream systems, and even lower hydraulic conductivities. The detrital material that makes up the Manitou Falls sandstones is composed of 95–100% of well-rounded quartz with minor muscovite and no feldspar.

Sandstones of the basal Manitou Falls Formation of the Athabasca Group are unconformably overlain by a succession of less-permeable marine sandstones, phosphatic siltstones, and phosphatic mudstones. These marine units in conjunction with the unconformities would be ideal environments in which evaporated seawater could permeate into the lower units. The Athabasca Group sedimentary rocks and the basement complex are cut by a series of northwest-trending mafic dikes, which were emplaced along reactivated fractures during post-Athabasca tectonic activity at 1270 Ma (LeCheminant and Heaman, 1989).

The maximum age of the Athabasca is constrained by the timing of rapid exhumation of the Trans-Hudson orogenic belts to the east of the basin at 1750 Ma (Alexandre et al., 2009; Kyser et al., 2000), whereas the minimum age comes from dates of 1640–1620 Ma for early diagenetic fluorapatite in the Wolverine Point Formation (Rainbird et al., 2007). The Athabasca Basin has been interpreted as an intracontinental basin as there is no evidence that the region was associated with mafic magmatism and rifting.

Unconformity-related uranium deposits can be classified on the basis of associated metals. Simple deposits have a simple mineralogy of uraninite, and complex deposits are polymetallic and have a diversity of sulfides and arsenides along with the uraninite (e.g., Thomas et al., 2000). Simple deposits tend to be hosted in fractures and faults in the basement more than 50 m below the unconformity and are comprised primarily of uraninite (**Figure 5**). In contrast, complex deposits are hosted by clay-altered Athabasca Group sandstones and conglomerates. The McArthur River deposit, the largest high-grade deposit in the world, is hybrid, being comprised of one basement-hosted and three basin-hosted ore bodies so far, with the basement-hosted P2 ore body containing about half of the uranium in the total deposit (McGill et al., 1993).

Detailed paragenesis of alteration minerals in the Athabasca Group and basement rocks forms a basis for all other studies and deposit models (Kotzer and Kyser, 1995). Detrital fluorapatite, monazite, and zircon occur within detrital quartz grains but rarely as detrital interstitial minerals, indicating that these heavy minerals have been removed by fluids flowing through the sandstone (Fayek and Kyser, 1997). Kaolinite and muscovite with minor amounts of montmorillonite and chlorite were also minor detrital components in the basin (Hoeve and Quirt, 1984; Kotzer and Kyser, 1995).

In basin-hosted deposits, pre-ore alteration is manifest as illite preceding minor pyrite and rutile, indicating reducing conditions, followed by chlorite and minor euhedral quartz formed in open fractures. The later ore stage is characterized by disseminated uraninite grains with chlorite rims or with no other minerals, and the post-ore stage by kaolinite and some spherulitic dravite, pyrite, rutile, and Cu, Ni, and Co sulfides.

With few exceptions, alteration assemblages of all basement-hosted deposits are generally the same. The earliest alteration phase involves intense illitization of feldspar, biotite, and amphibole followed by alteration of biotite and illite to chlorite. Illite is dominant distal to the ore zone, whereas chlorite is dominant proximal to the ore body. Initial uranium mineralization is manifest as uraninite, with illite as the only phase that accompanies uraninite precipitation. Post-ore alteration is manifest as vein chlorite, euhedral quartz, spherulitic dravite, dolomite, and kaolinite. Pyrite, rutile, and rare chalcopyrite, bornite, pentlandite, cobaltite, and magnetite precipitate late as disseminated euhedral to subeuhedral grains.

Basement-rooted faults were important for focusing mineralizing fluids in these deposits and for later alteration events (e.g., Hoeve and Sibbald, 1978), although the vast majority of faults are not mineralized. Reactivated faults rooted in the basement and initially associated with the Trans-Hudson orogen offset the unconformity by hundreds of meters, and a few are associated with mineralization (Baudemont and Pacquet, 1996). In the McArthur River area, ore pods are localized where cross faults intersect the P2 fault (Györfi et al., 2007), with mineralization mainly in reverse faults along graphitic units and quartzites.

Isotopic compositions, phase relations, and fluid inclusion characteristics indicate that the basinal fluid throughout the basin underwent physical and chemical increases relative to the fluid present when the early quartz overgrowths formed, evolving from 15 to 30 wt% NaCl and from 120 to 250 °C, and becoming more ^{18}O-rich (Hiatt et al., 2007; Kyser et al., 2000). These changes resulted from increasing burial depth and sustained water–rock interactions with the basinal sediments over substantial time periods. These fluids were oxidized, pH-neutral, saline basinal brines capable of leaching uranium from detrital phases in the sandstones and transporting uranium (Kotzer and Kyser, 1995). In addition to the uranium sourced by basinal brines interacting with detrital minerals in the basins, alteration of monazite in basement rocks is another possible source (Hecht and Cuney, 2000).

Pre-ore alteration occurred around basement- and basin-hosted deposits beginning at 1670 Ma, but the major uranium mineralization event occurred at 1600 Ma based on U/Pb dates of uraninite and Ar/Ar dates of syn-ore illite and is the same throughout the basin for both basement- and basin-hosted deposits (Alexandre et al., 2009; Holk et al., 2003). Several subsequent fluid events affected all the minerals in the structurally hosted deposits and moved radiogenic Pb into the areas around the deposits (Holk et al., 2003). The ages of these events correspond to far-field effects from the Mazatzal orogeny at 1600 Ma, the Berthoud orogeny at *c.*1400 Ma, the Mackenzie dike swarms at 1270 Ma, the Grenville orogeny at 1100 Ma, and the assemblage and breakup of Rodinia up to 850 Ma. Given that the major uranium mineralization event occurred 150 My after the basin began to form, the basin architecture and hydrogeology at that time are critical to understand what factors controlled the formation of the deposits.

13.19.5.1.2 The Kombolgie Basin

The Kombolgie Basin is located on the Arnhem Land plateau area and is the northern part of the larger McArthur Basin in the Northern Territory of Australia (Figure 7). In contrast to the Athabasca Basin, all the deposits so far in the Kombolgie Basin are basement-hosted, although in the McArthur Basin, deposits such as the Westmoreland (Polito et al., 2005a) are associated with intrusive units in the basin fill.

The Paleo- to Mesoproterozoic McArthur Basin is filled with a thick (5–15 km) sequence of nearly flat-lying sedimentary rocks interpreted to have formed in terrestrial and marine environments. Volcanic rocks deposited on the North Australian craton periodically punctuate these sedimentary successions and are indicative of rifting periods, as in the Kombolgie Basin. The sedimentary fill is intruded by the Jimbu Microgranite and the Oenpelli Dolerite at 1720 Ma, and subsequent magmatic episodes are characterized by minor intrusions of phonolitic and doleritic dikes that occurred between 1370 and 1200 Ma (Page et al., 2000).

The Kombolgie Basin is floored by Archean gneisses and intrusions and Paleoproterozoic intrusions and metasedimentary units (Figure 7). Overlying the intrusives and steeply dipping basement metasediments is the relatively undeformed and flat-lying Kombolgie Subgroup, which consists of sandstone, conglomerate, and interlayered volcanic units. Economic deposits of uranium have primary mineralization ages of 1650–1680 Ma (Polito et al., 2011) and are hosted in the Paleoproterozoic basement rocks near the unconformity. The Kombolgie Subgroup is composed of at least three stratigraphic sequences (Hiatt et al., 2007), each comprised of basal coarse-grained sandstones deposited in high-energy braided river systems, followed by quartz arenites that exhibit much better sorting and represent deposition in much lower-energy distal braided streams and overlain by well-sorted, medium-grained quartz arenite representing aeolian dune deposition. The top of each sequence has tidal deposits and a basal volcanic unit. Basin subsidence or sea level rise late in the depositional history of the Kombolgie results in marine conditions with evaporites that eventually evolved into mineralizing fluids.

The Jabiluka unconformity-related uranium deposit comprises Jabiluka 1 with a resource of 1.3 Mt of ore grading 0.20% U and Jabiluka 2 with a resource of 31.1 Mt grading 0.45% U and 3.07 g t^{-1} Au. The deposit was discovered in 1971 but has never been mined, unlike the strikingly similar nearby Ranger deposits (Figure 3). Mineralization is hosted by shallow-to-steeply dipping Paleoproterozoic basement rocks comprising graphitic units of chlorite–biotite–muscovite schist of the Cahill Formation (Figure 6). Jabiluka sits on the southwestern margin of the Myra High, which probably had a paleotopographic shoulder in the vicinity of the Jabiluka deposit, thus projecting potential reducing lithologies into diagenetic aquifers. The uranium mineralization is structurally controlled within brittle shears that are subconformable to the basement stratigraphy and breccias that developed within the hinge zone of fault-related folds adjacent to the shears (Polito et al., 2005b).

Jabiluka has an alteration halo in the basement rocks that extends at least 200 m beyond the known uranium ore (Binns et al., 1980). Alteration associated with uranium mineralization can be loosely divided into an outer and inner halo, with

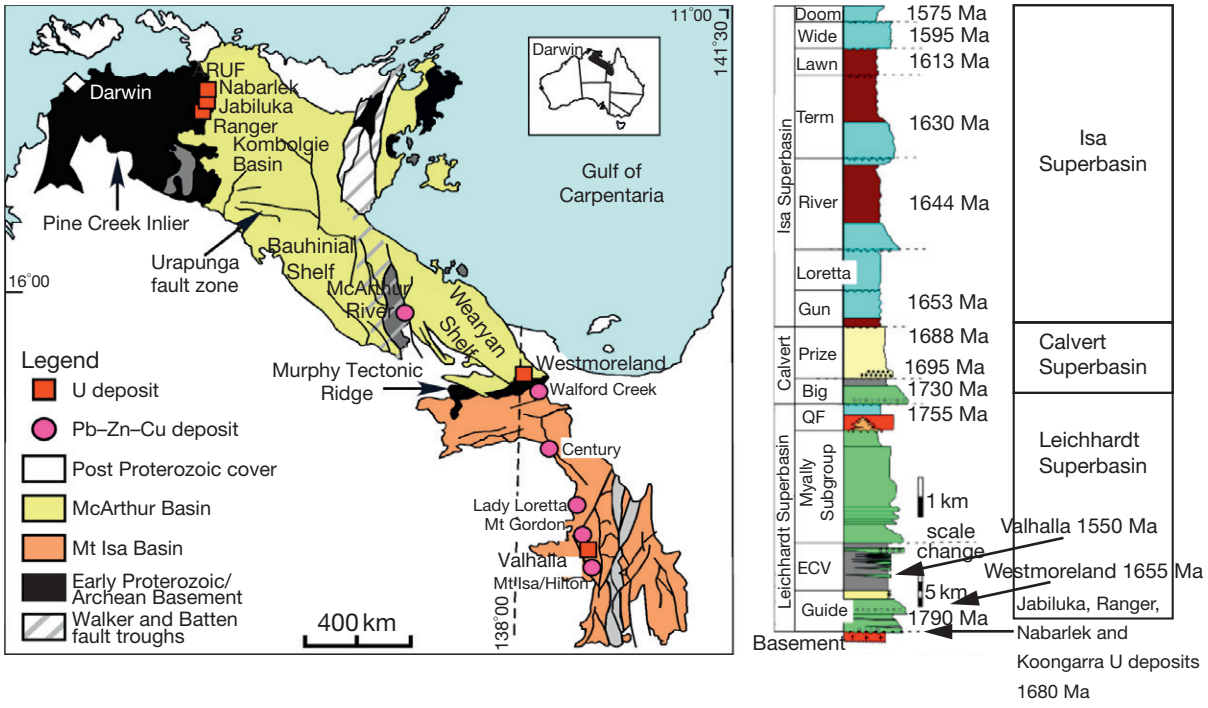

Figure 7 Left: Generalized geologic map of the Mt Isa and McArthur basins showing locations of Zn–Pb–Ag, Cu, and unconformity-related uranium deposits. The Kombolgie Basin is the northwestern part of the McArthur Basin. Right: Generalized stratigraphic sequence of the Mt Isa and McArthur River basins showing the stratigraphy of the three superbasins, ages of the units determined from U–Pb dates of felsic volcanics or detrital zircons, and stratigraphic positions of unconformity-related uranium deposits and their ages.

the principle difference being an increase in fine-grained chlorite and sericite associated with brecciation in the inner halo. Alteration in the outer halo at Jabiluka is represented by chlorite that pseudomorphs most metamorphic minerals, but metamorphic zircon, muscovite, quartz, and carbonaceous graphitic material are not visually altered in this area despite the alteration of adjacent phases.

Uraninite is the dominant uranium mineral at Jabiluka and is intimately associated with chlorite, sericite, and hematite. Crosscutting relationships show that multiple generations of uraninite cut chlorite and vice versa. Uraninite also occurs with sericite and euhedral quartz in high-angle crosscutting veins. Syn-ore illite and chlorite record mineralization temperatures of 200 °C and fluids identical to those in diagenetic aquifers that occur in the Kombolgie Subgroup. Massive uraninite first precipitated at 1680 Ma during brine migration and was subsequently altered by later fault-controlled fluid movement.

A scenario proposed by Polito et al. (2005b) that adequately explains the paragenesis of minerals in the deposit involves basinal fluids in diagenetic aquifers being drawn into the reducing basement after faulting and brecciation, thus precipitating uraninite and other alteration minerals. The basinal fluids equilibrate with the basement, and those that did not hydrate the basement assemblage are driven into the sandstone during compression related to increased stress postfailure. These Mg-rich fluids precipitate chlorite until the next rupturing event occurs and fluids are again drawn into the basement.

Another deposit in the area, Nabarlek, is hosted by Paleoproterozoic amphibolite schists on the north side of the Myra High. In contrast to most other unconformity-related deposits, no graphite was present in the host lithologies, suggesting that Fe^{2+} was the reductant. Uranium mineralization is associated with an inner and outer alteration halo that extends as far as 1 km from the Nabarlek fault. Alteration in the outer halo began as early as 1700 Ma and is dominated by chlorite and sericite, which formed when a 200 °C fluid flowed into the Nabarlek fault from the overlying Kombolgie Subgroup (Polito et al., 2004). Massive uraninite precipitated from the same fluids at *c.*1640 Ma and formed together with illite and hematite at *c.*200 °C. Chlorite was not coeval with uraninite, unlike at Jabiluka.

13.19.5.1.3 Karku, Russia

The Pasha–Ladoga Basin in western Russia is located in a depression created by the intersection of two major fault zones in a horst-and-graben structure, with the Karku unconformity-related deposit located over a block uplifted by 200–300 m from surrounding basement rocks (Velichkin et al., 2005). The Ladoga Supergroup basement rocks are mafic schists, amphibolites, and granite gneisses dated at 2100–1800 Ma and deformed during the Svecofennian orogeny at 1900–1800 Ma (Velichkin et al., 2005). The large Salmi rapakivi granite pluton intruded the basement rocks at 1530–1547 Ma at the northeastern edge of the basin.

The Riphean Pasha–Ladoga Group basin rocks consist of the basal Priozerskaya Formation with lower sandstone and upper flood basalt members dated at 1499 ± 68 Ma (Andreeva and Golovin, 2005). Overlying this is the Salminskaya Formation with lower sandstone and upper flood basalt members, then conglomerates and siltstones of the Pasha Formation, and finally unconsolidated Quaternary glacial moraine sediments.

High-grade ore zones up to 19% U occur within the sandstone near the unconformity. Mineralization is associated with illite–smectite mixed-layer minerals (Velichkin et al., 2005), which is unlike other unconformity-related deposits. Syn-ore calcite fluid inclusions and illite clay crystal chemistry indicate deposit temperatures of 170–300 °C, a level of heating at which smectite layers in the interstratified clays should have been destroyed (Freed and Peacor, 1989). Uraninite occurs as a complete replacement of the matrix minerals and postdates the chlorite. The uraninite has been dated by U–Pb Secondary Ion Mass Spectrometry at 1405 ± 76 Ma (Shurilov et al., 2006) and laser ablation inductively coupled plasma mass spectrometry at 1467 ± 39 Ma.

The Karku deposit appears to be unconformity-related but is different from the Athabasca and Kombolgie basins in several key aspects. The age of the basin itself is younger, having formed during the Mesoproterozoic after emplacement of underlying Kapakavi granites at 1530 Ma (Andreeva and Golovin, 2005). Moreover, the sediments in the area of Karku are immature, feldspathic, clay- and lithic-rich sandstones and conglomerates with significant amounts of calcite cement, distinct from the clean arenites of the Athabasca and Kombolgie basins. Karku records the same temperatures and basinal fluid sources as unconformity uranium deposits in Canada and Australia, but there is a lack of wide-scale circulation of mineralizing fluids in the deposit area itself as evidenced by the silicified, immature, clayey nature of the Priozerskaya Formation, which was an aquitard over the deposit. Perhaps fluids circulated through the deeper, basal paleoaquifers at depth, leached uranium into solution, flowed along the unconformity in response to the far-field tectonic event that caused extensive rifting and graben in the area, and focused into structures near the unconformity below the paleoaquitard unit.

13.19.5.1.4 Otish Basin, Quebec

The Paleoproterozoic Otish Basin and the related Mistassini Basin are located at the margin of the Archean Superior Province adjacent to the Grenville Front in central Quebec, Canada. Sedimentary fill lies unconformably on quartz–biotite–feldspar gneisses and migmatites, and metavolcanic and metasedimentary belts, including graphite schists of the Superior Province (Gatzweiler, 1987). These basement lithologies are intruded by NNW (north-northwest)-trending diabase dikes that date between 1926 and 2150 Ma, a maximum age for the basin, but the sedimentary fill in the basin was intruded by sills and dikes of the Otish Gabbro at 1730 Ma (Chown and Archambault, 1987), a minimum age for basin formation.

Sedimentary rocks of the Otish and Mistassini basins overlie a well-developed paleosol (Chown and Caty, 1983). Units of the Otish Basin include the basal Indicator Formation and the overlying Peribonca Formation. Chown and Caty (1973) suggested a terrestrial-dominated Otish Basin that laterally transitioned to a marine-dominated Mistassini Basin, with increasing marine influence in the Otish Basin through time. Conglomerate and sandstone sequences of the Indicator Formation record minimal early diagenetic compaction and cementation that allowed formation of regional diagenetic aquifers, with muscovite alteration due to interaction with seawater-influenced basinal brines at 250 °C (Beyer et al., 2012).

Gatzweiler (1987) described an unconformity-related deposit at Camie River, having geochemical associations with Cu, As, Ni, Co, Cr, and V, similar to complex-type deposits in the Athabasca Basin. Mineralization at Camie River occurred at 1721 ± 20 Ma (Beyer et al., 2012), which coincides with the 1730 Ma Otish Gabbro intrusion that promoted circulation of uranium-bearing basinal brines. Uranium in the basinal brines at Camie River was reduced by basement-hosted massive sulfides, although graphite is also present. The basinal brines produced coarse-grained chlorite and tourmaline and neoformed phengitic muscovite when reacting with the Otish Gabbro, which decreased the fluid-conducting capabilities of diagenetic aquifers and resulted in fracture-controlled fluid flow during much of the mineralizing process. Metamorphic fluids from the proximal 1100 Ma Grenville metamorphism had little effect at Camie River because of low water/rock ratios.

There are over 150 Proterozoic basins preserved globally, with many prospective based on what is known about the origin of these deposits. However, our level of knowledge is still missing some critical factors that would allow us to be predictive. Among these are the source of the uranium, the nature of an effective trapping mechanism, and the critical flux of the fluids involved. All of these affect exploration strategies indirectly and must be addressed in future endeavors. Given the high grade and size of unconformity-related deposits, evaluating each with appropriate regional and deposit criteria may yield significant payoffs.

13.19.5.2 Sandstone Uranium Deposits

Sandstone-hosted uranium deposits are defined as epigenetic concentrations of uranium minerals occurring as impregnations and replacements primarily in fluvial, lacustrine, and deltaic sandstone formations (Finch and Davis, 1985). The deposits occur in medium- to coarse-grained sandstones deposited in a continental fluvial or marginal marine sedimentary environment. Impermeable shale/mudstone units are interbedded in the sedimentary sequence, normally just above and below the mineralized sandstone. Uranium precipitated under reducing conditions caused by a variety of reducing agents within the sandstone, including carbonaceous material (detrital plant debris, amorphous humate, and marine algae), sulfides (pyrite and H_2S), hydrocarbons (petroleum and humate), and interbedded mafic volcanics. The deposits range in age between the Paleozoic and Tertiary and, less commonly, Proterozoic. Typical sedimentary environments conducive to their formation include molasse-like sequences in fluvial–lacustrine systems on wide forelands between a subduction zone and an intracratonic sea, intermontane basins in foreland regions, and fluvial–shoreline systems of marginal marine plains (Everhart, 1985).

Sandstone deposits constitute about 25% of world uranium resources (**Figure 1**). Ore bodies of this type are commonly low-to-medium grade (0.05–0.4% U) and individual ore bodies are small to medium in size, ranging up to a maximum of 50 000 tU (OECD/NEA-IAEA, 2008, 2010). The main primary uranium minerals are uraninite and coffinite. Conventional mining/milling operations of these deposits have been progressively undercut by cheaper in situ recovery (ISR) mining methods.

There are four main types of sandstone deposits (**Figure 8**):

- *Basal-type deposits* occur in poorly consolidated, highly permeable, fluvial-to-lacustrine carbonaceous gravels and sands deposited in paleovalleys directly incised in basement rocks, generally granitic, and capped by plateau basalts or sediments.
- *Tabular deposits* are irregular, elongate lenticular bodies parallel to the depositional trend, commonly occurring in palaeochannels incised into underlying sediments.

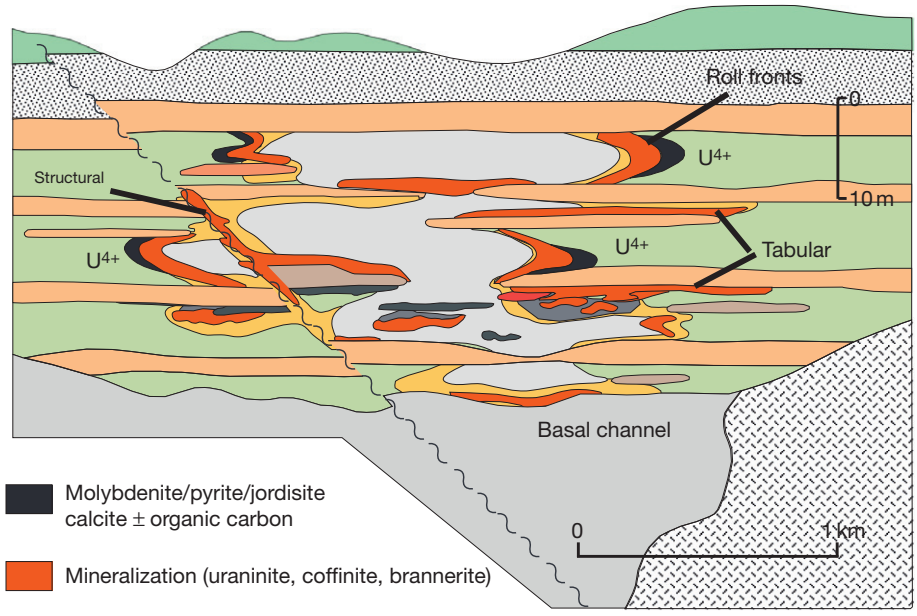

Figure 8 An idealized section showing the distribution and occurrence of three of the major types of sandstone uranium deposits and the distribution of oxidized and reduced sandstones. Reproduced from IAEA (2009) *World Distribution of Uranium Deposits (UDEPO) with Uranium Deposit Classification*, *IAEA TECDOC 1629*. Vienna: International Atomic Energy Agency.

- *Roll-front deposits* are arcuate bodies of mineralization that crosscut sandstone bedding.
- *Tectonolithologic deposits* occur in sandstones adjacent to a permeable fault zone but are also controlled by paleochannels and roll fronts. Some place collapse breccia-type deposits in this category, but they are separate in this chapter.

The two main uranium deposit forms are tabular and roll front, which are the focus of this section. Most sandstone-hosted uranium deposits are strikingly similar, despite occurring in host rocks ranging from Carboniferous to Tertiary and on almost every continent (Finch and Davis, 1985). The deposits in Ordovician and Devonian host rocks are syngenetic and related to carbonaceous black shale, but the dominant occurrences in Silurian and younger host rocks reflect the development of vascular land plants, the primary source of the reductant for fixing uranium from groundwaters. The timing of the mineralizing process is closely related to the diagenesis of the host rock, which in turn is related to the tectonic evolution of the area. In continental platform and intracratonic basins, Carboniferous, Permian, Jurassic, and Cretaceous tabular deposits are found in Argentina, Brazil, Niger, South Africa, and the United States. Intermontane basins in Australia and the United States host Tertiary roll-front deposits, whereas graben and regional extensional basins in India, Japan, and the United States host Permian, Triassic, and Tertiary tabular- and basal-type deposits. Volcanogenic basins host relatively young Tertiary and Quaternary tabular deposits in Italy and Mexico, and continental margin basins in Brazil, France, India, and the United States contain roll-front, tabular, and tectonolithologic deposits hosted in Devonian, Permian, Cretaceous, and Tertiary sandstones.

Most of the basins that host these deposits were essentially on stable cratons or their margins and closed to the sea, which prevented wholesale oxidation and promoted reducing conditions during and after sedimentation that was essential for uranium deposition. Adjacent elevated provenance terranes resulted mostly in high-energy fluvial systems of variably permeable sediments that restricted groundwater flow and concentrated the uranium. Primary ores were precipitated in host rocks near their initial dips, and in younger host rocks, these have not been modified. In pre-Tertiary host rocks in some regions, such as the San Juan Basin, USA, tectonic uplift and exposure of the margins of basins allowed introduction of oxidizing groundwater to redistribute tabular ores as roll fronts and in faults. In other areas, such as the San Rafael District in Argentina, folding and faulting the original host-rock beds into steeply dipping beds did not redistribute the ore minerals, whereas in others, such as Lodève in France, primary ores were redistributed into fractures and breccia zones. Clearly, paleoenvironment, tectonics, and paleohydrology had to be optimal to create and preserve these deposits.

13.19.5.2.1 United States

The Grants uranium region of the San Juan Basin includes five major uranium districts distributed over an area of 150 km by 30 km on the southeastern Colorado Plateau in northwestern New Mexico. Although mining has slowed, the deposits and geology have been well studied and so serve as a basis of knowledge. Within the region is the Ambrosia Lake district, the largest uranium-producing area in the United States, with 238 000 mt U estimated total resources (Finch and Davis, 1985). The deposits are tabular sandstone-type in which the uranium is associated with redistributed carbonaceous material such as humate. During Late Jurassic time, three broad alluvial fans were deposited in the basin upon Middle Jurassic sediments. The fans constitute the Morrison Formation and Salt Wash Member in the north and the Recapture and Westwater Canyon–Brushy Basin members in the south. The Morrison Formation was partly eroded in the south during the Upper Cretaceous before being unconformably transgressed by the Dakota Sandstone and the Mancos Shale. The Laramide orogeny (Cretaceous/Tertiary) resulted in the Zuni Mountains in the south, northward tilt of the Morrison Formation, and Tertiary volcanics of Mt Taylor that cover the Mesozoic sediments.

Tabular uranium deposits in the Westwater Canyon and Brushy Basin sandstone mineralized lenses are reduced or rereduced presumably from the humate formed from soluble organic substances during diagenesis. Early alteration of volcaniclastic material resulted in clays that preceded and partly overlapped the reduction process in the ore hosts. The humic material subsequently precipitated with the uranium and barite; calcite and kaolinite crystallized in pores within the sands. Mineralized trends have been strongly altered, with corroded quartz, altered plagioclase, albite and K-feldspar cements, and mixed-layer illite–smectite or chlorite. Chlorite is enriched in the ore zone, and kaolinite and altered montmorillonite are enriched updip from the ore. Primary ore consists of coffinite and black amorphous uranorganic complexes interstitial to the sand grains, along with pyrite, marcasite, and jordisite. Uranium is associated with enrichments of Cu, Fe, Mn, Mo, Se, V, Y, As, S, and organic carbon. Primary mineralization has U/Pb dates of 140–130 Ma (Brookins, 1980; Rosenberg and Hooper, 1982). Mobilization occurred at 115–110 Ma, perhaps associated with a first roll-type ore formation and almost continually thereafter (Ludwig et al., 1984).

The sediment pile provided a particular chemical environment due to the juxtaposition of two inherently unstable components, organic material in the form of plant debris and volcanic glass within the tuffaceous intercalations. Groundwaters within the Westwater Canyon Member were relatively oxidized compared to the organic-rich alkaline and reducing waters of the Brushy Basin Member. Along this interface, the primary uranium–humate mineralization of the Grants uranium region probably precipitated (e.g., Adams and Saucier, 1981). Bacteriogenic H_2S and carbon dioxide from fermentation of the vegetation would cause a drop in pH, altering the silicates and precipitating pyrite and uranium, the latter from uranyl carbonate and uranyl humate complexes. The favorable site for this process is the mudflat facies of the Brushy Basin Member (Turner-Peterson and Fishman, 1986).

Major roll-front uranium districts in Wyoming include the Wind River, Shirley, Powder River, and Great Divide basins. The Wyoming basins are the second major uranium producers in the United States after the Colorado Plateau, with total reserves of 250 000 mt U at 0.05–0.25% U. Significant roll-front uranium deposits are hosted in the early Eocene formations. The most favorable host rocks are friable fine to coarse-grained or pebbly, arkosic sandstones containing considerable pyrite and carbonaceous material. The host

sandstones are in the central part of the fluvial system in large fans that range in length from a few kilometers in the Wind River and Shirley basins to 100 km in the Powder River Basin. Sandstone-hosted uranium deposits in the Shirley Basin in Wyoming have U/Pb ages that indicate significant post-formational interaction with fluids, but the best age for the formation of these deposits is 24 Ma for the youngest ore and >35 Ma for the oldest ore (Ludwig, 1979).

Calcite-cemented ore has the highest grades of up to 12% U. Pyrite has been added to reduced sandstone at the edges of the altered sandstone tongues, as has selenium. Molybdenum is concentrated at the distal, downdip edge of the mineralized zone, and V has been deposited on the convex side of the roll front. Organic carbon has an erratic distribution, sulfate is high in mineralized sandstone, and phosphate is related to high uranium contents. U/Pb dates vary from 22 to 35 Ma (Ludwig, 1978, 1979) as the apparent mineralization times. The two most probable sources for the uranium are uraniferous granitic rocks of Lower Proterozoic to Archean age exposed in the ranges that surround the uranium-bearing basins in Wyoming and uraniferous tuffs and bentonitic volcaniclastic sediments of the Eocene and of younger age that overlie or once overlaid the basins.

13.19.5.2.2 Africa

The Paleoproterozoic Franceville Basin is located about 500 km SE of Libreville, Gabon, and is sandstone-hosted, although distinct from other deposits in terms of its age and occurrence. All deposits occur along the southwestern edge of the basin adjacent to the Massif du Chaillu (Gauthier-Lafaye and Weber, 1989). Total reserves are 42 700 mt U at an average grade of 0.3% U (OECD/NEA-IAEA, 2008, 2010). The Franceville Basin was formed as an intracratonic structural depression during the Paleoproterozoic in the Archean basement of granites and gneisses in the Massif du Chaillu. The intracratonic Francevillian sedimentary series is divided into five formations, FA to FE, and is 1000–4000 m thick. The lowermost formation, FA, rests unconformably on the Archean basement, hosts all of the uranium deposits in the basin, and consists of basal quartz-pebble conglomerates and coarse-grained arkosic sandstones that grade progressively upward into medium- to coarse-grained sandstones with dolomitic matrix. The FA formation is transgressed by the FB formation, which consists of up to 1000-m-thick black carbonaceous marine shales carrying kerogen and bitumen. The FC to FE formations are composed of shale, chert, dolomite, and volcanic rocks. The series is overlain by Mesozoic continental sediments of the Congolian basin.

The uranium deposits were formed by multistage events around 2050 Ma, about the same time as early diagenesis of the Francevillian sedimentary series (Mathieu et al., 2001). During maximum burial, reducing fluids in the form of oil migrated from the black shales into the upper part of the FA sandstone. At the same time, oxidized fluids in the permeable FA sandstones leached uranium from detrital phases (Mathieu et al., 2001). A tectonic event uplifted the basin, hydrofracturing the sandstone to produce secondary porosity and permeability. Uranium was deposited as uraninite by the mixing of oxidized basinal brines with the reduced fluids from the overlying FB formation (Mathieu et al., 2001). All of the uranium deposits of the basin appear to be located in fracture zones and tectonic structures, and all have kerogen or bitumen and pyrite and galena, with minor marcasite and chalcopyrite, digenite, and covellite. Mineralization occurs in lenses 20 m long and 10 m wide and 2 m thick. Very high-grade mineralization occurs at Oklo as lensoid bodies of up to 80% uraninite in a clay gangue, approximately 10 m long (Gauthier-Lafaye et al., 1989). The natural reactors of the Oklo area are a unique phenomenon among the uranium deposits of the world. They are characterized by a depletion of ^{235}U from 0.72% to between 0.62 and 0.296% and trace fission products.

Tabular uranium deposits in the Late Permian lower Beaufort Group and Late Triassic Molteno and Elliot formations within the main Karoo Basin generally contain less than 1000 tU of 0.08% recoverable U grade, although the estimated resource totals 31 000 tU. They share many of the same characteristics as the deposits in the United States and are known to occur in the greater Karoo Basin in Malawi and Tanzania. Uranium-bearing solutions moved through the sand bodies and precipitated uraninite (and coffinite) when they interacted with sparse reduced zones of carbonaceous debris.

13.19.5.2.3 Asia

Sandstone-type uranium deposits occur throughout northwest China in the Mesozoic to Cenozoic basins that are part of the network of basins that stretch from China into Kazakhstan, Mongolia, and Siberia (Zhou et al., 2000). The Sanerlin uranium deposit in southern China is early Tertiary in age and located near the margin of the Chaling–Yongxing Basin (Li et al., 2002), a pull-apart basin. The ores occur as breccias and veins mixed with silicified shale and sandstone. Uraninite occurs as disseminate grains within quartz veins or coatings on fragments. Fluid inclusions in the quartz veins have homogenization temperatures of 150–280 °C and variable salinities of 5.6–13.4 wt% NaCl. Isotopic compositions of the mineralizing fluids indicate that they were basinal brines from the Chaling–Yongxing Basin. Precipitation of uraninite is proposed to have occurred when carbonaceous gases were released from the ore fluids due to hydraulic fracturing.

The Olov and Ima uranium deposits in the Transbaikal region of Russia occur along the flanks of Jurassic depressions between granite gneiss domes and the intersection of major lineaments. The deposits are stratiform and controlled by low-dipping faults developed near the contact between the Jurassic volcanogenic and sedimentary rocks with the underlying granitoids. The paleovalleys that host the bodies are of variable age and are altered by pre-ore clay minerals and syn-ore biotite. Hematization is widespread, resulting from the mixing of ascending reduced hydrothermal fluids with near-surface oxidized water.

In 2008, Kazakhstan became the world's second largest producer of uranium after Canada and is poised to become the world's largest producer (IAEA, 2009). The Moinkum deposit complex in the southern part of the Chu-Sarysu Basin, which is typical of the emerging resource in Kazakhstan, is located in a regional depression and is related to an upper Paleogene monoclinal flexure that formed NW- and NE-trending anticlines and synclines. Mineralization is hosted in Cretaceous and Palaeocene/Eocene arkosic sandstones deposited by NNW flowing river systems that originated in the Tian Shan Mountains,

500 km to the south. Roll-front systems developed at the interface between oxidized and reduced sandstones, resulting in individual roll fronts that range in length from 300 to 15 000 m and in width from 50 to1600 m. The average ore grade of the Moinkum deposit complex is 0.06% U as coffinite associated with Fe- and S-rich organic matter and Se, Rh, Mo, Sc, Co, and Ni. These occur as a coating on detrital grains, as veinlets inside organic lithoclasts, as disseminated minerals, and in the silty–clayey cement and are leached by ISR with sulfuric acid. The reductant here is proposed to be the same as the roll fronts in Texas, namely hydrocarbons (Jaireth et al., 2008).

13.19.5.3 Vein Deposits

Vein deposits occur as veins in metamorphic (and other) rocks, commonly contain deposits that do not fit into other types, and have origins that are complex (Martin-Izard et al., 2002; Ruzicka et al., 1995). Vein deposits constitute 7% of the global reserves and about 10% of world uranium production. Major deposits include Beaverlodge (Canada), Jáchymov (Czech Republic), and Shinkolobwe (Democratic Republic of the Congo), all of which have been mined out. The Beaverlodge deposits represent the most complex of these and therefore serve as a model for how these deposits may form.

13.19.5.3.1 Beaverlodge, Canada

The Beaverlodge area in the central–southern Archean Rae Province, northwestern Saskatchewan, Canada, is located just north of the Athabasca Basin and is the host of numerous fault-controlled uranium deposits (Tremblay, 1978). Various 'types' of deposits have been identified, ranging from intrusive–metasomatic at Gunnar to breccia-related in the major deposits. Uranium mineralization occurs primarily in basement Murmac Bay Group rocks, which have been affected by at least four episodes of deformation coincident with major orogens in the area. Metamorphic facies range from amphibolite to granulite, with partial anatexis leading to granitization, such as at the Gunnar deposit. The Murmac Bay basement rocks and a thin regolith lie beneath the Paleoproterozoic successor Martin Lake Basin that is stratigraphically older than, but is spatially related to, the younger uranium-rich Paleoproterozoic Athabasca Basin. The Martin Lake Basin is filled with volcanic and clastic rocks. The age, tectonic setting, and origin and characteristics of the fluids that formed the uranium deposits in the Beaverlodge area have been a subject of controversy for decades.

Paragenetic relationships of minerals in uranium deposits in the Beaverlodge area reveal that there are six distinct periods and styles of uranium-mineralizing events associated with multistage deformation during the Proterozoic (Dieng et al., 2011). The Saint Louis fault, which is proximal to the most significant deposits at Ace–Fay–Verna and the Cinch Lake deposit, records evidence of exhumation and episodic structural reactivation at progressively shallower crustal levels, accompanied by hydrothermal alteration and the distinct stages of uranium mineralization. Two minor early stages near 2350 Ma are associated with cataclasite rocks and early tensional quartz–calcite ± uraninite veins, coincident with the late stage of the Arrowsmith orogen. Following emplacement of the Gunnar granite at 2321 Ma, albite metasomatic alteration of the granite is associated with a third, moderate uranium-mineralizing event. The Gunnar-type mineralization is formed from Na–K–F ± Cl brines that exsolved from residual magmatic hydrothermal fluid at 300–400 °C and filled voids after quartz dissolution following Na metasomatism of the Gunnar granite. The style of the granite metasomatism is similar to the albitized granite-hosted uranium mineralization in Brazil. However, uranium associated with this metasomatic style of mineralization is overprinted by the more significant breccia-vein and later volcanic-type mineralization.

During the late Paleoproterozoic, exhumation along major faults caused the deformation style to change from dominantly brittle–ductile to brittle at shallower structural levels. Massive brecciation of preexisting rocks is associated with the fourth, and most significant, uranium-mineralizing event at 1848 ± 5 Ma from Ca–Na–F ± Cl fluids at 330 °C, coincident with peak regional metamorphism of the Trans-Hudson orogen. The breccia-vein mineralizing event occurs in all deposits, including at Gunnar. Alteration is restricted to near the deposits and consists of calcite, chlorite, sericite, hematite, and late albite veins.

With additional exhumation, deposition of sediments and volcanics in the Martin Lake Basin and emplacement of feeder alkaline mafic dikes are associated with the fifth, minor mineralizing event at 1823 ± 23 Ma. This minor event occurred from fluids from F–P_2O_5-rich magmatic fluids at 315 °C originating from magmatic–hydrothermal degassing along fractures during intrusion of feeder mafic dikes.

Late mineralized veins correspond to the sixth, minor mineralizing stage at 1620 ± 4 Ma, coincident with the Mazatzal orogeny and the major unconformity-related uranium-mineralizing events in the Athabasca Basin. The Athabasca-type mineralization is formed from oxidizing Ca–Na–F–Cl-rich basinal brines at 235 °C. This minor mineralization is only observed in the Ace–Fay and Martin Lake deposits. The age of the mineralization and composition of the mineralizing fluid are similar to those of the unconformity-related uranium deposits in the Athabasca Basin in Canada.

Vein-type deposits, which are always associated with breccias, are related to regional tectonic events along major crustal structures and 'metamorphic'-derived fluids. Although widespread, this style of mineralization rarely is significant enough to form large deposits.

13.19.5.4 Metasomatic Deposits

These deposits occur in structurally deformed rocks mainly altered by sodium or calcium metasomatism and hematization (Dahlkamp, 1993). The grades tend to be low, less than 0.17% U, and these deposits currently constitute 9% of the global reserves. Alkali metasomatism is a widespread yet poorly understood process that can be associated with uranium ore-forming processes. It is most commonly manifest as albite enrichment, with quartz dissolution in most cases. Albite enrichment can be related to (1) purely magmatic processes (Linnen and Cuney, 2005), wherein volatiles in extremely fractionated melts expand the stability field of quartz and shift eutectic melt composition toward albite (Manning, 1981); (2) hydrothermal–metasomatic processes, wherein fluids are exsolved from magmas; or (3) the final phases of regional metamorphism (Polito et al., 2009). Albitization may be pre- or syn-ore associated with regional deep structures.

Regardless, only a small proportion of the rocks altered by Na metasomatism normally contain uranium ore.

Uranium mineralization associated with Na metasomatism occurs primarily during two major tectonic events in earth history. The major one corresponds to the 1.9–1.7 Ga assemblage of megacontinents during which massive orogens associated with major regional metamorphism and igneous activity occurred at convergent plate margins (Cuney, 2010). Examples include the highly mineralized Krivoy Rog district in Ukraine, the Kurupung district in Guyana, and Liangshanguan in northeastern China. As the megacontinents themselves were assembled, another widespread Na–U metasomatic event at 1.4–1.5 Ga is recorded by deposits in the Lagoa Real district in Brazil and the Valhalla deposits in Queensland.

13.19.5.4.1 Na metasomatism-related deposits of Ukraine

The Krivoy Rog district is located within the Sarmatia craton, which, with the Fennoscandian and Volgo–Uralian cratons to the north, forms the east European craton. Sarmatia first joined with the Volgo–Uralia craton at 2000 Ma to form the Volgo–Sarmatia craton, during which all rocks within the suture zone underwent metamorphism, migmatization, and S-type granitic magmatism from 2050 to 2020 Ma. At *c.*1800 Ma, Fennoscandia joined the Volgo–Sarmatia craton.

Uranium mineralization associated with Na metasomatism in Ukraine is situated along several north–south, deeply rooted continental scale structures occurring between and within the blocks of the central part of Sarmatia. In the west where the city of Krivoy Rog is located, deposits are located within the Paleoproterozoic metasedimentary formations of the Krivoy Rog–Zheltorechensk syncline. Further to the east, the Michurinskoye, Severinskoye, and Vatutinskoye deposits are in the Kirovograd structure, which hosts high-grade metamorphic units and granites dated at *c.*2200 Ma. Even further east, the Novokonstantinovka structure hosts several deposits older than1800 Ma. The altered zones and uranium mineralization are controlled by ductile structures that were active at temperatures in excess of 500 °C. Deformation continues under brittle conditions with crystallization in fractures of euhedral albite capped by pitchblende. The ore bodies are lenticular, several meters wide, and hundreds of meters long and deep. Uranium mineralization is usually of low grade, generally 0.01% U, but can reach 0.3% locally, and total resources are estimated to be in excess of 100 000 tU. The deposits have been discovered by systematic drilling.

Sodium metasomatism in quartz–feldspar-bearing rocks has an outer barren zone in contact with the unaltered host rocks within which K-feldspar is albitized. The internal zone has quartz dissolution and albite and hematite that host the uranium mineralization. They correspond to nearly pure albitites with minor amounts of mafic minerals and ubiquitous hematite, magnetite, apatite, zircon, and rutile. Uranium is present as uraninite, brannerite, davidite, coffinite, and secondary hexavalent uranium minerals. Calcium metasomatism may occur in the internal alteration zone with formation of pyroxene, garnet, epidote, and carbonates.

Possible uranium sources in the deposits include protoliths with high initial uranium, such as orthogneisses or conglomerates with detrital uraninite. Metamorphic fluids derived from anatectic zones and ascending upward along deep and large fractures have been proposed as the source of the fluid, but there may be a difference of 200 My between regional metamorphism and the mineralizing processes. Alternatively, Na metasomatism and uranium mineralization may be related to late Proterozoic tectonic–magmatic activity along deep structures after peak metamorphism (Emetz et al., 2010).

13.19.5.4.2 Valhalla, Australia

The Valhalla uranium deposit, located 40 km north of Mt Isa (**Figure 7**), is one of 107 uranium occurrences that have been recorded in 1800–1700 Ma metasediments of the Leichhardt River Fault Trough (Neumann et al., 2006). The deposit is hosted in interbedded arkoses, sandstones, and siltstones within basalts belonging to the Eastern Creek Volcanic Group (1790 Ma) in the western part of the Mt Isa Basin. The Mt Isa Basin near the Valhalla deposit was metamorphosed to upper greenschist–amphibolite facies during the *c.*1550 Ma Isan Orogeny (Connors and Page, 1995), and therefore, this deposit has both a basinal and metasomatic origin.

The Valhalla deposit has an inferred resource of 7632 tU at 0.064% U, with brannerite the dominant ore mineral. The volcanic and sedimentary rocks hosting the uranium mineralization were first altered to albite, fluorine-rich magnesio-riebeckite, calcite, Ti–V-rich magnetite, and minor brannerite, uraninite, and dolomite in a strongly foliated rock. Then, the rocks were brecciated, further altered, and cemented by albite, riebeckite, calcite, apatite, hematite, anatase, brannerite, U-rich zircon, and uraninite, which represented the main mineralization.

Brannerite U–Pb and Pb–Pb dates are 1555–1510 Ma and overlap the $^{40}Ar/^{39}Ar$ ages of 1540 Ma obtained from early and main-stage riebeckite (Polito et al., 2009). These dates are coincident with the timing of peak metamorphism in the Mt Isa area during the Isan Orogeny.

The hydroxyl site of apatite and riebeckite within the ore zone contains a large proportion of fluorine, suggesting that fluoro complexes transported the uranium. Syn-ore coexisting calcite and riebeckite give apparent oxygen isotope equilibration temperatures of 340–380 °C for the mineralization stage. The isotopic composition, timing, and temperature of the mineralization event are most consistent with fluids derived from regional metamorphism of the proximal metasediments during the Mt Isan Orogeny, especially given the absence of syn-Isan granites in the western Mt Isa Basin (Polito et al., 2009).

Metasomatic-type deposits represent a potentially significant resource. Their geologic environment and timing is well known, as well as the origin of the fluids. However, areas that have been metasomatized by Na fluids rarely have uranium deposits, so critical elements for their formation are not understood.

13.19.5.5 Breccia Complex Deposits

Breccia complex deposits of uranium are exclusively the Mesoproterozoic (1590 Ma) Olympic Dam IOCG deposit, the world's largest individual deposit at about 2 200 000 tU, which occurs in a hematite-rich granite breccia complex in the Gawler craton (Direen and Lyons, 2007). IOCG deposits constitute 15% of the global reserves and 10% of the global production of uranium (along with vein-type deposits). They have the lowest grades and normally would not be considered as uranium deposits were they not polymetallic.

The Olympic Dam IOCG (U–Ag–REE) deposit is located on the Gawler craton, South Australia. Mineralization occurs in a hematite breccia complex hosted by the Roxby Downs Granite of the Hiltaba Granite Suite, dated at 1588 Ma (Creaser, 1996), and covered by a thick Mesoproterozoic to Cambrian sedimentary sequence of the Stuart Shelf. The Roxby Downs Granite represents the most fractionated member of the large Mesoproterozoic Burgoyne batholith of the Hiltaba Suite, a quartz–monzonite to granite suite typical of A-type, high-K calcalkaline granites and comagmatic with Gawler Range Volcanics (Oreskes and Hitzman, 1993). The breccia complex extends approximately over 7 km along a NW–SE direction and is zoned with a central barren quartz–hematite breccia associated with volcaniclastic rocks and a variably mineralized outer zone of hematite–granite breccia (Oreskes and Hitzman, 1993). Clasts of surficial sedimentary and volcaniclastic rocks are found within heterolithic breccias. Volcanic rocks range from lapilli tuffs to felsic porphyritic lavas, all with hematite alteration. Mafic to felsic dikes intrude the breccia complex as the final steps of the magmatic activity.

The typical alteration mineralogy with the uranium is sericite–hematite, minor chlorite, quartz, carbonate, and magnetite, and the intensity of alteration is generally linked to the extent of brecciation. The main uranium-bearing phases are uraninite, coffinite, and brannerite, but their paragenesis, timing, and character are wholly understudied. Uranium ore genesis is proposed to be related to the mixing of a hot, high-salinity fluid from a granitic magma, which subsequently mixed with an oxidizing meteoritic fluid (Oreskes and Einaudi, 1992). However, recent results indicate that there were sediments above the intrusion and prior to brecciation and that the hydrothermal system at Olympic Dam did not vent magmatic fluids (McPhie et al., 2011), so that basinal fluids may have been involved in the uranium mineralization.

Although these IOCG deposits do contain some uranium, it is normally a liability for the Cu and Au being extracted, and most IOCG deposits do not have elevated uranium contents. Olympic Dam is anomalous in this respect and normally would not be considered a uranium deposit because of its low grade, despite the large tonnage. The uranium must be removed so the Cu and Au can be marketed – the uranium is a bonus.

13.19.5.6 Intrusive Deposits

Intrusive deposits are associated with high-temperature concentrations of uranium in alaskite, pegmatite, granite, monzonite, and carbonatite. Major world deposits include Rössing (Namibia), Ilímaussaq (Greenland), Bokan Mountain (United States; **Figure 9**), and Palabora (South Africa). They tend to have low grades and comprise only 4% of the current global production. Uranium mineralization is related to magma composition (Cuney and Friedrich, 1987). The uranium deposits in alaskites and peralkaline granites are related to high-temperature magmatic processes, whereas the uranium deposits related to metaluminous and peraluminous are mainly related to lower temperature hydrothermal processes.

13.19.5.6.1 Alaskites

Deposits related to partial melting are those corresponding to uraninite enrichments disseminated in pegmatic dikes and injected into high-grade migmatitic gneisses. The Rössing deposit in Namibia is the most significant deposit related to partial melting processes, despite it being among the lowest-grade uranium deposits mined for uranium, at an average grade of about 300 ppm uranium but at a resource over 142 000 tU. The deposit is situated approximately 55 km northeast of Swakopmund in the Namibian desert. Several other deposits of the same type have been discovered nearby in similar geologic settings.

Granitoid dikes hosting the uranium mineralization at Rössing appear to be derived from the partial melting of uranium-rich sediments in the Damara Pan-African belt between the Omaruru and Okahandja lineaments. The Damara orogen resulted from a triple continental collision between the Kalahari craton to the north, the Congo craton to the south, and the São Francisco craton to the east. The central zone of the northeast branch comprises deformed rocks of the Damara sequence, resting uncomfortably on the Mesoproterozoic gneissic and volcanosedimentary Abbabis complex, which has a minimum age of 1038 Ma (Kröner et al., 1991). The metamorphic grade increases from east to west, reaching partial melting in the coastal area.

The collision between the Congo and Kalahari cratons resulted in a deformation including a 160-km-wide highly metamorphosed central zone where the Rössing deposit is located. The central zone records granulite facies conditions, partial melting, and development of NE-trending elongated domes. All uranium-bearing occurrences related to alaskites are in the southern central zone.

A sedimentary package was deposited in an epicontinental platform of a passive margin at 900–800 Ma on an E–W-oriented rift graben of the Abbabis complex. The 40-km-wide graben is mainly filled with high-energy siliciclastic sediments, rhyolites, and evaporites of the Nosib Group. In the Rössing area, the Nosib Group includes the continental to nearshore siliciclastic Etusis Formation to the gneisses of the Khan Formation. The Rössing dome corresponds to the partially melted Etusis Formation (Nex et al., 2001). Subsequently, marine sedimentation progressively invaded the entire Damara Basin.

Primary uranium mineralization is only in the felsic rocks, mainly located in the vicinity of the marbles of the Rössing Formation and amphibolites of the Khan Formation. Euhedral Th-bearing uraninite is the dominant ore mineral, with high and variable Ca contents reflecting the interaction of the alaskite melts with enclosing calcium-rich lithologies. A date of 508±2 Ma was obtained on zircons, monazites, and uraninite from an alaskite (Briqueu et al., 1980).

The origin of the mineralized leucocratic granite dikes of the Rössing type has been attributed to partial melting of uranium-rich metasediments or metavolcanics (Cuney and Barbey, 1982). The preferential accumulation of the alaskites in the vicinity of carbonate-bearing lithologies can be attributed to the production of carbon dioxide that reduced the water partial pressure, thereby shifting the solidus of the silicate melts to higher temperatures and freezing them preferentially at the level of the Rössing Formation (Cuney and Kyser, 2008).

Other alaskite occurrences include the Litsk area of the NE Kola Peninsula, Russia, which are related to Archean pegmatitic granite. The late orogenic potassic granites of southern Finland are strongly enriched in uranium and share many characteristics

with the Rössing alaskites, but accumulations large enough to form an economic deposit remain to be discovered. They were emplaced between 1.85 and 1.79 Ga along a 100-150-km-wide zone of Paleoproterozoic basement, extending from SW Finland to Russia and representing one of the most U–Th–K-enriched areas in Fennoscandia (Lauri et al., 2007).

13.19.5.6.2 Peralkaline systems

13.19.5.6.2.1 The Ilímaussaq complex

The Ilímaussaq intrusion is a peralkaline, silica-undersaturated plutonic complex situated in the eastern part of the 1.1–1.3 Ga Gardar province of South Greenland, where rifting at 1280 and 1180–1140 Ma produced large-scale melting of the asthenosphere that ponded at the crust–mantle boundary, resulting in a series of fractionated melts (Andersen et al., 1981). The igneous complex covers about 156 km^2 and comprises a diversity of granitic and syenitic rock types emplaced as three successive melt batches, which intruded and fractionated at depths of 3–4 km. The last batch corresponds to the intrusion of nepheline- and sodalite-bearing syenite from the same deep magma chamber as the first stage and small bodies of lujavrite, the most uranium-mineralized rocks in the uppermost structural level of the peralkaline complex. Mineralized lujavrites typically contain nepheline, eudialyte, sodalite, and clinopyroxene crystals enclosed in a mixture of albite and microcline.

The lujavrites represent the most fractionated melts and therefore are enriched in incompatible elements. Larsen and Sørensen (1987) propose a fractionation at the crust–mantle boundary of parental melts to the Ilímaussaq rocks, with successive 'leaking' responsible for the three magma batches rising to a high-level chamber where further crystal fractionation continues at 700–900 °C and 1.5 and 3.5 kbar. Although the earlier melts were reduced, with fO_2 below Quartz-Fayalite-Magnetite and methane as a stable fluid phase, fO_2 was buffered by arfvedsonite–aegirine and more oxidized in the late stages, consistent with successive magma batches derived from one continuously fractionating magma at depth.

13.19.5.6.2.2 Bokan Mountain (United States)

The Bokan Moutain U–Th deposit at Kendrick Bay (**Figure 9**), southeastern Alaska, is associated with a Late Jurassic peralkaline granite that intrudes Paleozoic metasediments and metavolcanics, quartz diorites, and quartz monzonites along the western side of the Chatham Strait fault. A U–Pb date for zircon of 171 Ma has been obtained for the post-tectonic Bokan Mountain granite (De Saint-Andre et al., 1983), a circular, multiphased, zoned intrusive. The ring structure is defined by a core of riebeckite–aegirine granite forming the main part of the pluton, surrounded by an aegirine granite and a border zone pegmatite. The Bokan Mountain granitic pluton is typically peralkaline. Variations in major element compositions do not reflect typical magmatic fractionation trends, but high contents of REE, Nb, and Zr are associated with some of the uranium zones (Thompson, 1988).

The first stage of alteration of the host aegirine granite resulted in albitization of K-feldspar and only weak mineralization. A second stage involved dissolution of quartz with simultaneous precipitation of albite and secondary pyrite and iron oxides. The U–Th mineralization is essentially hosted in these desilicified and albitized parts of the granite predominantly as uranothorite disseminated in the albite. Veins represent the second uranium resource at the Ross Adams deposit, extending to more than 2.5 km WNW from the Bokan Mountain pluton.

Enrichment in the mantle source regions in incompatible and high field strength elements (HFSE) through the subduction of oceanic slab with variable amounts of continental sediments considerably enhances the U and Th concentrations in the fractional derivatives that are generated. Fluid saturation of the melts leads to deposition of much of the U and Th as fluids are focused in a zone of weakness at the southeastern margin of the pluton, producing intense microfracturing and alteration of the granite. Alteration started with the albitization of K-feldspar and with increased fluid percolation, simultaneous quartz dissolution, and new albite growth as the fluid cools from magmatic temperatures of 700–600 °C down to 350 °C, the maximum solubility for quartz under low-pressure conditions. Fluids enriched in F, HFSE, and REE escaped into the host rocks along veins producing the vein-type mineralization. Fluid inclusions indicate carbon dioxide consistent with fluid unmixing and overpressurization that enhanced fracturing. In contrast to Ilímaussaq, the carbon dioxide phase is devoid of methane or higher hydrocarbons.

13.19.5.6.3 Peraluminous granites

Peraluminous leucogranites and volcanics occasionally host uranium deposits. These magmas can form directly from a high degree of partial melting of metagreywackes or metapelites at temperatures above 800 °C and dry conditions (Vielzeuf and Holloway, 1988). If they form from low degrees of partial melting of essentially quartz–feldspar-rich protoliths, further uranium enrichment in the melt and crystal fractionation will produce peraluminous uranium-rich granites, provided the ratio of HFSE/U is low in the restites and during fractionation. Enrichment in HFSE also occurs during fractional crystallization, but uranium, mainly as uraninite, requires extreme differentiation, forming too small a stock to represent sizable ore deposits.

Two mica peraluminous leucogranites are by far the most commonly associated with uranium deposits. The largest province of this type is the mid-European Variscan Belt with Carboniferous granites. The most fractionated members of the peraluminous granites are represented by rare metal, high-phosphorus, highly peraluminous granites or pegmatites (Lithium-Cesium-Tantalum; LCT type), extremely depleted in Th, Zr, and REE (Linnen and Cuney, 2005). The Th/U ratios of such granites decrease during fractionation.

The mid-European Variscan uranium province extends over more than 2000 km and represents a major U, Sn, W, and Au province in which uranium mineralization is related to granites derived from the partial melting of the continental crust during the collision between the Eurasian and African continental plates at *c.*400 Ma. The deposits are predominately Permian and located either in the granites, such as in the Massif Central and Brittany, or in their enclosing metamorphic rocks, such as in the Erzgebirge district. France has most of the uranium resources of western Europe as vein-type deposits in the Massif Central. There is no distinct temporal or spatial distribution of the different types of granites throughout the Variscan orogen. However, low–medium-K calcalkaline granites are never associated with uranium mineralization because most of the uranium is hosted by refractory accessory minerals and

high-K calcalkaline granites are not directly associated with the deposits in the Variscan Belt because the uranium is mainly hosted in uranothorite ($(U,Th)SiO_4$), which is very resistant to leaching when hydrothermal circulation occurred long after granite emplacement (Cuney and Friedrich, 1987).

A belt running from Limousin into Brittany has high heat production of 2.0–8.2 mW m^{-2} and a 15-km-thick layer of pre-Variscan formations enriched in radioelements by more than two times the average crust. The belt corresponds to a pre-Variscan feature. All two mica leucogranites enriched in uranium and having deposits are located within this high-heat flow-heat belt, which reflects partial melting of uranium-enriched metamorphic protoliths.

The uranium mineralization associated with peraluminous leucogranites in the Variscan orogen results from multistage processes, beginning with the late Proterozoic to early Paleozoic partial melting of a metasomatized mantle, followed by several stages of partial melting of metal-rich portions of the continental crust, and finally by hydrothermal circulation controlled by long-lived structures deeply rooted in the continental crust. Fluids involved in the genesis of the Variscan vein-type uranium deposits have low salinities with temperatures of 100–200 °C. Stable isotope studies indicate that uranium deposition results from the mixing between an oxidizing meteoric water able to leach uraninite from the enclosing granite and a connate fluid that infiltrated from overlying Permian formations and provided hydrocarbons or H_2S to reduce the uranium (Turpin et al., 1990).

13.19.5.7 Volcanic-Associated Deposits

Uranium deposits occur in felsic volcanic rocks in continental extensional settings and caldera complexes (Leroy and George-Aniel, 1992). The deposits are related to faults and shears within the volcanic units (Figure 9), and uranium is commonly associated with Mo, F, Th, and REE. They comprise 3% of the global uranium production and typically have grades of 0.04–4% U. These form from uranium-enriched felsic magmas that are subsequently affected by hydrothermal fluids, and they range in age from Proterozoic to Tertiary.

13.19.5.7.1 Streltsovkoye caldera (Transbaikalia, Russia)

The Streltsovkoye caldera is located near the eastern Russian–Chinese–Mongolian border. The caldera complex belongs to an Upper Jurassic–Cretaceous volcanic belt, which extends from Siberia to Kazakhstan, through Mongolia. The Streltsovkoye caldera represents the largest uranium ore field associated with volcanism in the world, with 18 deposits totaling ore resources above 0.2% U of more than 260 000 tU (Laverov et al., 1992). Little has been published on these deposits, and what is represented here is distilled from Cuney and Kyser (2008). The caldera has a diameter of about 20 km and was filled with basalts, andesites, trachydacites, rhyolites, and interlayered sedimentary horizons having a present thickness of more than 1 km. The caldera filling occurred during the Late Jurassic, starting with a basal conglomerate overlain by the Upper Jurassic Priargunski Formation of interlayered sediments and various volcanic rocks. These are overlain by the 155–135 Ma Turginski Formation of rhyolites, ignimbrites, and a few basaltic horizons and capped at 135 Ma by conglomerates, sandstones with coal intercalations, and thin layers of basalts and andesites of the Kutinsky Formation. The main volcanic centers are located at the intersection between the NE or NS extensional faults and NW faults. The basement is mainly composed of Precambrian metamorphic formations and Paleozoic granitoids.

Uranium mineralization is located in any of the different volcanosedimentary horizons and in the granitic basement so that the main control of ore deposition is structural (Figure 9). Mineralization generally occurs as subvertical or horizontal veins or stockworks, and all enclosing rocks are altered. Uranium contents average about 0.15 wt%, up to 0.6 wt% in large stockworks and up to 1.0 wt% in veins. The major deposits inside the Streltsovkoye caldera are the Tulukuevskoye open-pit and Streltsovkoye–Antei underground mines.

The Streltsovkoye–Antei deposit is a vein-type mineralization hosted in the volcanic rocks and the basement. It is the most important deposit with resource estimates greater than 60 000 tU. The vein thickness varies from a few meters up to 60 m. The Streltsovkoye deposit is composed of six interconnected mineralized bodies along NS and NE structures, mainly hosted by trachyandesitic tuffs, whereas the Antei deposit is entirely located in the granitic basement along vertical NS structures at depths of 350–1400 m.

The Streltsovkoye deposit records a first stage of local albitization in the deep part of the deposit and intense illite–phengite and chlorite alteration dated at 133 Ma by K–Ar (Chernyshev and Golubev, 1996). Temperature estimates of the pre-ore stage are 280–300 °C. During the quartz–pitchblende–brannerite syn-ore stage at 135 Ma, mineralizing fluids had temperatures up to 460 °C and Na–Cl–HCO_3 compositions that transported U^{6+} as chloride or fluoride complexes. A decrease in the fluid temperature was the main cause of the ore deposition. Brannerite ores occur at depths of more than 1300 m in the basement, mixed pitchblende–coffinite–brannerite ores between 800 and 1300 m, and molybdenite–pitchblende ores at higher levels.

The sources for the uranium deposits from the Streltsovkoye include peralkaline rhyolites filling the caldera, fluids expelled from the underlying magma chamber, subalkaline granitoids in the basement, and preexisting Ordovician uranium mineralization. The rhyolitic tuffs, which represent 35 vol% of the volcanic pile, have enough U, Zr, and F to explain the total resources of all the deposits of the Streltsovkoye caldera (Chabiron et al., 2001). Magmatic fluids are lower than the estimated resources of the Streltsovka caldera, although they could have enriched the granites of the basement along fractures and formed the high-temperature brannerite mineralization in the deepest part of the ore system. Both the high-K granites in the basement, with metamict accessory minerals, and the preexisting uraninite in the Ordovician could have been leached by hydrothermal-magmatic fluids.

Other uranium districts occurring in caldera-like structures developed within cratonic areas and characterized by U–Mo–F associations include the Dornot caldera in northeastern Mongolia, the Xiangshan caldera in southeastern China, the U–Mo Kitts-Michelin deposit in Labrador, Canada, the U–Mo mineralization in Tertiary rhyolites of the Sierra Peña Blanca, Mexico, and the U–Mo in Carboniferous ignimbrites at Ben Lomond deposit, Queensland, Australia.

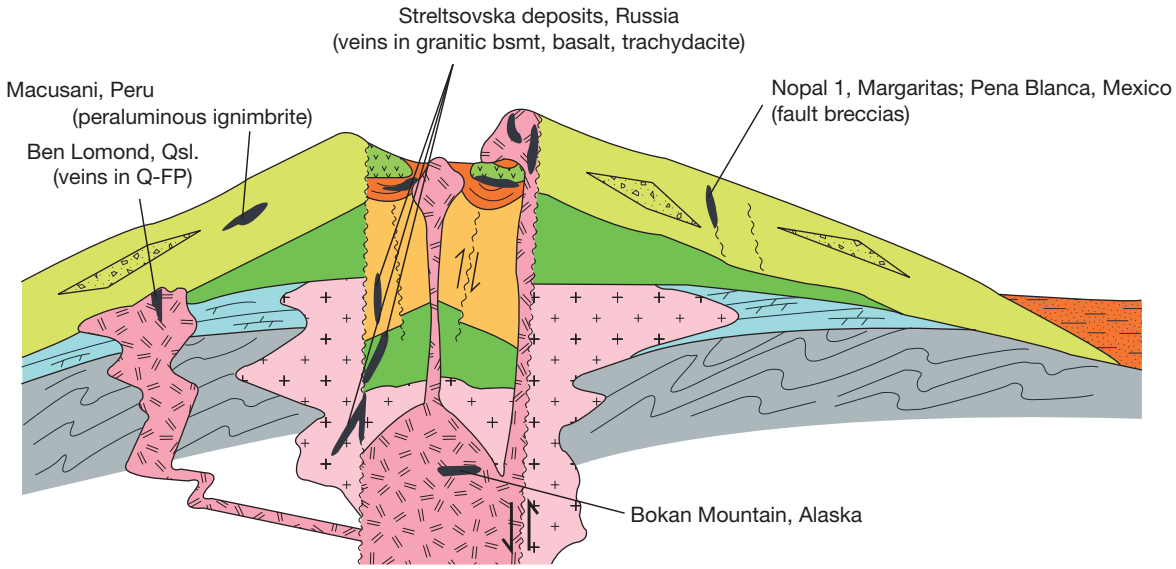

Figure 9 Location of various volcanic-associated uranium deposits in igneous systems. Reproduced from IAEA (1985) Uranium deposits in volcanic rocks. *Proceedings of a Technical Meeting, El Paso*, TX, United States, 2–5 April 1984, 468 pp, Vienna: International Atomic Energy Agency.

13.19.5.7.2 Macusani, Peru

Strongly acidic, highly peraluminous volcanics equivalent to the two mica peraluminous leucogranites are quite rare (Figure 9). The only well-known occurrence associated with uranium mineralization are the Macusani volcanics in Peru, which occur in the upper part of a 1400-m-thick pile of strongly peraluminous ignimbritic ash-flow tuffs (17–4 Ma) emplaced synchronously with small Tertiary peraluminous granite stocks (27–8 Ma) (Cheilletz et al., 1992). These rhyolites have the same composition as the peraluminous leucogranites with about the same level of U enrichment (up to about 20 ppm) and depletions in Th, Zr, and REE. They represent a potential source of uranium via devitrification of the glass by oxidizing fluids. Uranium mineralization occurs as a primary autunite along with Mn oxides and phosphates, but no uraninite. Fluid isotopic compositions are consistent with precipitation at low temperatures from meteoric waters. Reserves are estimated in excess of 8500 tU.

13.19.5.8 Quartz-Pebble Conglomerate Deposits

Quartz-pebble conglomerate uranium deposits are defined as stratiform and stratabound deposits of uraninite and brannerite hosted in pyrite-rich quartz-pebble conglomerates. Pyrite is the main detrital and authigenic heavy mineral, with pyrite contents generally between 3 and 15%. These deposits are hosted by the basal sequences of Archean and Paleoproterozoic basins and can be of detrital or hydrothermal origin. They make up approximately 2% of the world's uranium resources. Where uranium is recovered as a by-product of gold mining, such as the Witwatersrand Basin, the grade may be as low as 0.01% U, whereas in deposits that were mined exclusively for uranium, average grades range as high as 0.15% U. Individual deposits range in size from 5000 to 160 000 tU.

There are two main types of quartz-pebble conglomerate uranium deposits. Elliot Lake-type deposits have mineralization affected mainly by sedimentologic controls. The ores grade from U through Th to Ti rich with decreasing pebble size and increasing distance from their source. Although brannerite is an alteration mineral, postdiagenetic remobilization is minimal and subordinate to sedimentologic controls. In contrast, Witwatersrand-type deposits have ores controlled by local chemical environments, such as along unconformities, shale and siltstone beds, and carbonaceous seams.

13.19.5.8.1 Blind River–Elliot Lake district

The Blind River–Elliot Lake district is located in southern Ontario at the southern margin of the Canadian Shield to the north of Lake Huron. The geology comprises Archean basement of metavolcanics, metasediments, and granitic and gabbroic intrusions; Paleoproterozoic Huronian Supergroup and post-Huronian intrusives; Paleozoic sediments; and Pleistocene to Recent glacial deposits. The Huronian Supergroup is a thick clastic sequence with minor tholeiitic basalts. At its base, the Elliot Lake Group consists of psammites and volcanics and includes uraniferous quartz-pebble conglomerates within the middle and lower portions of the Matinenda Formation, which is the lowermost unit of three similar cycles in the Huronian Supergroup (Mossman et al., 1993). The Lower Huronian section contains pyrite associated with uranium in nearshore clastic units. The Upper Huronian contains thorium and abundant hematite that has been cited as evidence for an increase in the level of atmospheric oxygen. A regional structure is the Murray fault, a high-angle reverse fault, north of which all economic deposits are located.

Postdepositional modifications of the Matinenda Formation include pressure solution of quartz, quartz cementation, sericitization of K-feldspars, and pyritization, with more than about 90% of the pyrite present being of postdepositional origin (Robinson and Spooner, 1984). Intrusion of Nipissing diabase dikes and sills caused local albitization, chloritization, and carbonatization of the wall rocks.

Principal ore minerals are uraninite, brannerite, and monazite, with minor coffinite, uraniferous kerogen, uranothorite, xenotime, and gummite (Mossman, 1999). The U/Th ratios in milled ore range from 2 to 3, typical of igneous sources. Uraninite grains are up to 0.2 mm and occur primarily as small clusters of grains between pebbles and in monomineralic subparallel bands of well-sorted angular grains concentrated proximal to the base of small-scale depositional units. Uranium content correlates with maximum apparent quartz-pebble diameter (Theis, 1979) and pyrite. Heavy minerals in the Matinenda Formation conglomerates give U/Pb dates of *c.*2500 Ma, indicative of an Archean source.

A syn-sedimentary placer deposit modified by postdepositional processes generated by diagenesis or mild metamorphism is the most cited model for these deposits (Robertson, 1989). Uraninite grains are rounded in a way that is best explained by fluvial transport and abrasion. The age and character of most of the uraninite are consistent with derivation from uraniferous Archean granites and pegmatites.

13.19.5.8.2 The Witwatersrand Basin

The Witwatersrand Basin is located along the border between the Orange Free State and the Transvaal. The Witwatersrand Basin covers an area of almost 50 000 km^2 underlain by more than 8000 m of slightly metamorphosed strata of the Dominion Group and Witwatersrand Supergroup, which host the ore-bearing, quartz-pebble conglomerates, and the Ventersdorp Supergroup, which is slightly mineralized. The lowermost sediment unit is the 3080 Ma Dominion Group (Frimmel and Minter, 2002), a 40–100-m-thick package of conglomerates, arkoses, and quartzites capped by lavas, tuffs, and shale with a composite thickness of almost 2700 m. Uranium occurs within the basal section in two oligomictic quartz-pebble conglomerates, the lower reef and the upper reef. The lower reef forms narrow lenses within paleovalleys incised into the Archean basement, and the upper reef, in contrast, is laterally more continuous.

The overlying 2.970–2.837 Ga Witwatersrand Supergroup is divided into a lower West Rand Group, about 4500 m thick, and an upper Central Rand Group, about 2500 m thick. The West Rand Group includes shales, quartzites, occasional conglomerates, and andesitic lavas, but uranium occurs in only one zone of the conglomerates. The Central Rand Group contains predominantly medium- to coarse-grained quartzites and conglomerates that host the most important uraniferous reefs comprising more than 80% of the total uranium. Uranium grade of in situ ore is generally very low, ranging from 0.013 to 0.06% U.

The principal ore minerals are uraninite, manifest as detrital grains with a degree of roundness similar to detrital monazite, uraniferous phyllosilicates in concretionary pyrite nodules, authigenic minerals of U–Ti phases, and uraniferous carbonaceous matter. Uranium accumulated as a matrix constituent in conglomerates, in pyritic sands, in quartzites along unconformity surfaces, and in carbonaceous bands on or adjacent to unconformity surfaces.

Uraninite grains from Witwatersrand ores have apparent U/Pb dates of 3065 ± 100 Ma, similar to the age of the granites surrounding the Witwatersrand Basin, and a secondary age of 2040 Ma that is coeval with the emplacement of the Bushveld Complex and the large Vredefort impact structure. The uraninite grains have up to 10% ThO_2, which is typical for uraninites from granites and pegmatites. However, Law and Phillips (2006) challenged the placer model for the genesis of the Witwatersrand deposits by suggesting that postburial fluids during diagenesis, deformation, and metamorphism were responsible for remobilization of the gold and the uranium. As is true of most things in complex natural systems, the truth is most likely between these extremes.

13.19.5.9 Surficial Uranium Deposits

Surficial deposits are broadly defined as young (Tertiary to Recent), near-surface uranium concentrations in sediments or soils that form primarily in hot climates (Otton, 1984). The environments in which they are found include nonpedogenic valley fill and playas; pedogenic, ephemeral, evaporative, karst caves; wetland valley fill and lacustrine deposits; tropical deposits developed in lateritic weathering profiles over uranium-rich source rocks; supergene enrichment of primary uranium ore bodies; epigenetic uranium entrapped in redox fronts above sulfide ore bodies; and alkaline lakes.

Terrestrial carbonate deposits currently comprise only about 1% of world uranium resources. They generally form where uranium-rich granites or acidic volcanic units were deeply weathered in a semiarid climate. Major uranium deposits in Western Australia (Lambert et al., 2005) occur in valley-fill sediments along Tertiary drainage channels and in playa lake sediments that overlie the Archean granite and greenstone basement of the northern portion of the Yilgarn craton (**Figure 10**). The uranium mineralization is carnotite (hydrated potassium U vanadate). In addition to Australia, uraniferous valley-fill deposits also occur in Namibia, South Africa, Mauritania, Somalia, Argentina, and China.

Calcretes, which host most surficial deposits, develop over several thousand years, initially in the form of nodules and becoming a massive, laminar horizon as the calcrete matures (Carlisle, 1984). Calcrete-hosted uranium deposits have relatively large tonnages but very low grades, with the average deposit size being 3000 tU at less than 0.05% U, except at Yeelirrie, which has reserves of 50 000 tU at a grade of 0.13% U. The principal alteration of the host rocks at Yeelirrie is hydrology related, leading selectively to the formation of calcrete, dolocrete, and other duricrust facies by the gradual replacement of kaolinite and quartz with dolomite, calcite, gypsum, and celestite. The replacement processes were associated with an increase in rock volume provoking small-scale folds, faults, ubiquitous slickensides, and diapiric structures or mounds bounded by faults.

The general model for the formation of surficial carbonate-hosted uranium deposits involves liberation of uranium from source rocks by leaching with slightly alkaline and oxidizing groundwaters and it being carried as uranyl carbonate complexes until fixation mechanisms intervene. At Yeelirrie, granitic rocks, anomalous in uranium content, served as the source for U, and V is probably derived from mafic minerals in the granitic rocks or greenstones (Butt et al., 1984). The basin that hosts the deposits had a low-relief, low-drainage gradient, large catchment area (**Figure 10**), including deeply

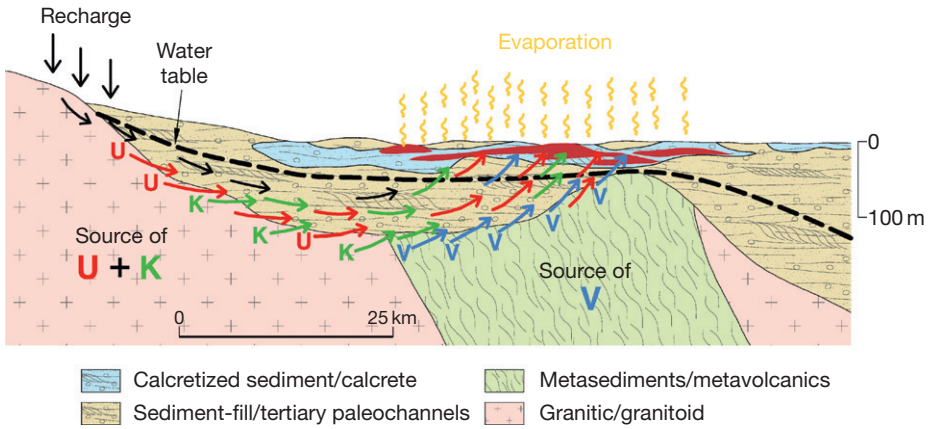

Figure 10 An idealized model of a calcrete-hosted deposit, such as Yeelirrie and others in arid climates in Western Australia. In the Langer Heinrich deposit in Namibia, the source of the vanadium is black shales.

weathered granitic rocks. Various fixation mechanisms for uranium in surficial deposits involve dissociation of uranyl carbonate species through the loss of CO_2, evaporative concentration of the solute species in near-surface groundwaters, change in the valence state of V or U, mixing of waters, and sorption by organic matter, silica, iron oxyhydroxides, and clay.

The major gaps in our knowledge about terrestrial carbonate uranium deposits that inhibit effective exploration are why are there only a few high-grade deposits, such as the Yeelirrie deposit in Australia, what controls the formation of the carnotite ore mineral, and how can deposits be imaged at a depth given that current techniques can only detect mineralization near the surface. Although most deposits to date are Recent in age, there is a paucity of studies on what makes calcretes definitive indicators of uranium mineralization and whether these environments in the distant geologic past can preserve uranium deposits.

13.19.5.10 Collapse Breccia Pipe Deposits

These deposits occur uniquely in Arizona and are hosted in a sequence of limestone, sandstone, and shale (Wenrich et al., 1995). The deposits average about 0.5% U, second to unconformity-related deposits in terms of grade. They have properties that are somewhat akin not only to sandstone deposits but also to unconformity-related systems.

Thousands of solution-collapse breccia pipes occur in the Grand Canyon region of Arizona because of the widespread Paleozoic carbonate and gypsum-rich rocks amenable to karsting. Breccia pipes are hosted by Mississippian to Lower Triassic stratigraphic units of almost horizontally bedded marine to marginal limestones, mudstones, and sandy to silty sediments (Wenrich et al., 1995). Roof collapse of caverns (paleokarst) in the carbonate strata of the Mississippian Redwall limestone initiated the formation of a pipe. The generally circular collapse transgressed chimney-like upward into the overlying, essentially flat-bedded sediments from the Redwall limestone to the Upper Triassic Chinle Formation.

The ore bodies can be divided into five stages, beginning with carbonates and sulfate minerals followed by metallic sulfides in stages two and three and then uranium in stage four. The uranium precipitated as uraninite along with calcite and minor copper sulfides. The main event occurred at 200 Ma and a minor event occurred prior to the deposition of the Chinle Formation at 160 Ma (Ludwig and Simmons, 1992). Most models invoke reduced brines within the limestones and containing base metals mixed with oxidized uranium- and copper-bearing groundwaters that were circulating in the sandstones (Wenrich et al., 1995). The uranium was transported as a uranyl carbonate complex, and effervescence of CO_2 with associated pressure release helped to break up uranyl compounds. Invading hydrocarbons containing H_2S derived from sediments surrounding the pipe may have been the agent for the required reduction of the U^{6+} ions, and coeval oxidation of some pyrite to hematite associated with the uraninite may be evidence of reduction by Fe^{2+}. Fluid inclusion studies suggest that the ore-forming solutions that deposited the sphalerite, calcite, and dolomite had minimum temperatures in the range of 80–173 °C, with salinities most commonly >18 eq wt% NaCl (Wenrich and Sutphin, 1989).

13.19.5.11 Phosphorite Deposits

Phosphorite deposits form from the upwelling of nutrient-rich marine waters onto a shallow continental shelf with sometimes restricted circulation (see Piper and Perkins, **Chapter 13.12**). Although the grades can reach 0.065% U and the resource is substantial, the uranium is also associated with other elements, such as Se and As, and the waste would be an environmental problem. Up to 900 t $year^{-1}$ were mined from the Florida phosphates, mainly during the 1980s. Currently, no phosphates are mined for uranium, but uranium is recovered unofficially from phosphates used for the production of fertilizers by several countries, and most countries do not report uranium from phosphorites as a resource. Reserves of uranium from phosphorite deposits are dominated by those from Morocco, although reported reserves are conservative because of the connotation of uranium being present in commercial fertilizers. Recent estimates reach 22 million tU globally (OECD/NEA-IAEA, 2008, 2010). Notwithstanding the problems associated with extracting the uranium and other elements from phosphorites, these deposits represent a significant reservoir of

uranium that may be more strategic in the near future as environmental demands for the removal of uranium from phosphates become more pronounced.

13.19.5.12 Black Shale and Seawater

Black shales and seawater also represent significant reserves of uranium, although economic extraction of uranium from each is a challenge. Uranium in shales resides with organic matter. The uranium contents of black shales are variable but can reach 400 ppm, such as in the Ranstad deposit in Sweden. Exploration for black shale deposits is currently in progress in several countries, with consideration for a mix of metals in addition to uranium. Significant reserves of uranium have been reported from the Chattanooga (United States) and Ronneburg (Germany) black shales, totaling nearly 4.2 million tU (OECD/NEA-IAEA, 2010).

The uranium concentration of seawater is only 3.2 ppb, but the quantity of uranium is substantial, about 4 billion tonnes. Research on an extraction process being developed in Japan suggests that it might be feasible to recover uranium from seawater at a cost of US$300/kg of uranium.

13.19.6 Synopsis

The uniqueness of uranium geochemistry as a redox reactive element, the need for uranium as a special resource, the variable geologic context of uranium-mineralizing processes throughout earth history, and the effects of tectonics on the uranium cycle all conspire to shape the models of deposit formation and preservation (Cuney, 2010). Twelve styles of mineralization were examined in this chapter by focusing on the most significant deposits. Many deposits, if not all, are not amenable to simple classification because most involve multiple processes. Uranium mineralization is driven in large part by redox reactions so that deposits that predate oxygenation of the atmosphere are magmatic because aqueous forms of uranium were minimal. Tectonics has played a critical role in the style of mineralization through subduction as a process to concentrate uranium in partial melts, through occasional formation and preservation of vast sedimentary basins, and by facilitating the evolution of the biosphere so that reactive reductants could accumulate. However, critical processes in how these deposits form and where they can be found are missing because the models are not really predictive but can be with an enhanced understanding.

Acknowledgments

The author would like to thank Steve Scott for presenting this opportunity to summarize the character of the major uranium deposits through the eyes of uranium geochemistry. Michel Cuney is thanked for his expert insights into uranium deposits, which, although sometimes different from mine, are always inspirational. This chapter was greatly improved by the comments of Steve Scott, Paul Alexandre, and Mostafa Fayek who took the time and care to review it constructively.

References

Adams SS and Saucier AE (1981) Geology and recognition criteria for uraniferous humate deposits, Grants uranium region, New Mexico. *Final Report US Department of Energy GJBX-2*(81).

Alexandre P, Kyser K, Thomas D, Polito P, and Marlat J (2009) Geochronology of unconformity-related uranium deposits in the Athabasca Basin, Saskatchewan, Canada and their integration in the evolution of the basin. *Mineralium Deposita* 44: 41–59.

Andersen S, Bohse H, and Steenfelt A (1981) A geological section through the southern part of the Ilímaussaq Intrusion. *Rapport Grønlands Geologiske Undersøgelse* 103: 39–42.

Andreeva OV and Golovin VA (2005) Altered wall rocks in the Karku unconformity-type uranium deposits and their genesis (northern Ladoga region, Russia). *Geology of Ore Deposits* 47: 410–428.

Ansolabehere S, Deutch J, Driscoll M, et al. (2003) *The Future of Nuclear Power, 175 pp.* Cambridge, MA: MIT Press.

Baudemont D and Pacquet A (1996) The Sue D and E uranium deposits, northern Saskatchewan: Evidence for structurally controlled fluid circulation in the Athabasca Basin. In: Ashton KE and Harper CT (eds.) *MinExpo'96 Symposium – Advances in Saskatchewan Geology and Mineral Exploration Saskatchewan Geological Society Special Publication 14, pp. 85–94*. Regina, SK: Saskatchewan Geological Society.

Becquerel AH (1896) On the invisible rays emitted by phosphorescent bodies. *Comptes Rendus Hebdomadaires des Séances de l'Académie des Sciences* 122: 501–503.

Beyer SR, Kyser K, Hiatt EE, Polito PA, Alexandre P, and Hoksbergen K (2012) Basin evolution and unconformity-related uranium mineralization: The Camie River U prospect, Paleoproterozoic Otish Basin, Quebec. *Economic Geology* 107: 401–425.

Binns RA, Ayres DE, Wilmshurst JR, and Ramsden AR (1980) Petrology and geochemistry of alteration associated with uranium mineralization at Jabiluka, Northern Territory, Australia. In: Ferguson F and Goleby AB (eds.) *Uranium in the Pine Creek Geosyncline, IAEA Proceedings Series*, pp. 417–438. Vienna: International Atomic Energy Agency.

Briqueu L, Lancelot J, Valois JP, and Walgenwitz F (1980) Géochronologie U–Pb et genèse d'un type de minéralisation uranifère: Les alaskites de Goanikontes (Namibie) et leur encaissant. *Bulletin des Centres de Recherche Exploration-Production Elf-Aquitaine* 4: 759–811.

Brookins DG (1980) Geochronologic studies in the Grants Mineral Belt. In: Rautman CA (ed.) *Geology and Mineral Technology of the Grants Uranium Region 1979 New Mexico Bureau of Mines and Mineral Resources Memoir* 38, pp. 52–58. Socorro, NM: New Mexico Bureau of Mines and Mineral Resources.

Burns PC (1999) The crystal chemistry of uranium. *Reviews in Mineralogy* 38: 23–90.

Butt CRM, Mann AW, and Horwitz RC (1984) Regional setting, distribution and genesis of surficial uranium deposits in calcretes and associated sediments in Western Australia. In: *Surficial Uranium Deposits: Report of the Working Group on Uranium Geology Organized by the International Atomic Energy Agency, IAEA-TECDOC-322*, pp. 122–127. Vienna: International Atomic Energy Agency.

Card C, Portella P, Annesley I, and Pană D (2007) Basement rocks of the Athabasca Basin, Saskatchewan and Alberta. In: Jefferson CW and Delaney G (eds.) *EXTECH IV: Geology and Uranium EXploration TECHnology of the Proterozoic Athabasca Basin, Saskatchewan and Alberta. Geological Survey of Canada Bulletin* 588, pp. 533–555. Ottawa, ON: Geological Survey of Canada.

Carlisle D (1984) Surficial uranium occurrences in relation to climate and physical setting. In: *Surficial Uranium Deposits: Report of the Working Group on Uranium Geology Organized by the International Atomic Energy Agency, IAEA-TECDOC-322*, pp. 25–35. Vienna: International Atomic Energy Agency.

Cawood PA, Nemchin AA, Strachan R, Prave T, and Krabbendam M (2007) Sedimentary basin and detrital zircon record along East Laurentia and Baltica during assembly and breakup of Rodinia. *Journal of the Geological Society* 164: 257–275.

Chabiron A, Alyoshin AP, Cuney M, et al. (2001) Geochemistry of the rhyolitic magmas from the Streltsovka caldera (Transbaikalia, Russia): A melt inclusion study. *Chemical Geology* 175: 273–290.

Cheilletz A, Clark AH, Farrar E, Arroyo Pauca G, Pichavant M, and Sandeman HAI (1992) Volcano-stratigraphy and $^{40}Ar/^{39}Ar$ geochronology of the Macusani ignimbrite field monitor of the Miocene geodynamic evolution of the Andes of southeast Peru. *Tectonophysics* 205: 307–327.

Chernyshev IV and Golubev VN (1996) The Strel'tsovskoe deposit, Eastern Transbaikalia: Isotope dating of mineralization in Russia's largest uranium deposit. *Geokhimiya* 10: 924–937.

Chown EH and Archambault G (1987) The transition from dyke to sill in the Otish Mountains, Quebec; relations to host-rock characteristics. *Canadian Journal of Earth Sciences* 24: 110–116.

Chown EH and Caty JL (1973) Stratigraphy, petrography and paleocurrent analysis of the Aphebian clastic formations of the Mistassini-Otish Basin. Special Paper, In: Young GM (ed.) *Huronian Stratigraphy and Sedimentation*, *Geological Association of Canada Special Paper*12, pp. 49–71. St. John's, NL: Geological Association of Canada.

Chown EH and Caty J-L (1983) Diagenesis of the Aphebian Mistassini regolith, Quebec, Canada. *Precambrian Research* 19: 285–299.

Connors KA and Page RW (1995) Relationships between magmatism, metamorphism and deformation in the western Mount Isa Inlier, Australia. *Precambrian Research* 71: 131–153.

Creaser RA (1996) Petrogenesis of a Mesoproterozoic quartz latite-granitoid suite from the Roxby Downs area, South Australia. *Precambrian Research* 79: 371–394.

Cuney M (2010) Evolution of uranium fractionation processes through time: Driving the secular variation of uranium deposit types. *Economic Geology* 105: 553–569.

Cuney M and Barbey P (1982) Mise en évidence de phénoménes de cristallisation fractionnée dans les migmatites. *Comptes Rendus de l'Academie des Sciences, Série IIA* 295: 37–42.

Cuney M, Brouand M, Cathelineau M, et al. (2003) What parameters control the high grade -large tonnage of the Proterozoic unconformity related uranium deposits? In: Cuney M (ed.) *Uranium Geochemistry 2003*. *Proceedings of International Conference,* Nancy, France, April 2003, pp. 123–126.

Cuney M and Friedrich M (1987) Physicochemical and crystal-chemical controls on accessory mineral paragenesis in granitoids – Implications for uranium metallogenesis. *Bulletin de Minéralogie* 110: 235–247.

Cuney M and Kyser K (2008) Hydrothermal uranium deposits related to igneous rocks. In: Cuney M and Kyser K (eds.) *Recent and Not-So-Recent Developments in Uranium Deposits and Implications for Exploration Mineralogical Association of Canada Short Course Series*, vol. 39, pp. 117–160. Quebec, Canada: Mineralogical Association of Canada.

Dahlkamp FJ (1993) *Uranium Ore Deposits*. Berlin: Springer-Verlag.

De Saint-Andre B, Lancelot JR, and Collot B (1983) U-Pb geochronology of the Bokan Mountain peralkaline granite southeastern Alaska. *Canadian Journal of Earth Sciences* 20: 236–245.

Dieng S, Kyser K, and Godin L (2011) Tectonic setting, fluid history and genesis of uranium mineralization in the Beaverlodge area, Saskatchewan, Canada. *Geological Association of Canada, Mineralogical Association of Canada (GAC-MAC) Annual Meeting,* Ottawa, ON, Canada, 25–27 May 2011.

Direen NG and Lyons P (2007) Regional crustal setting of iron oxide Cu-Au mineral systems of the Olympic Dam region, South Australia; insights from potential-field modeling. *Economic Geology* 102: 1397–1414.

EIA (2007) *International Energy Outlook*. Washington, DC: Department of Energy.http://www.eia.doe.gov/oiaf/ieo/index.html.

Emetz AV, Sherbak DM, Vyshnevsky OA, and Cuney M (2010) Conditions of formation of uranium deposits related to sodium metasomatism in Ukraine. In: Williams PJ, et al. (ed.) *Smart Science for Exploration and Mining, Proceedings of the 10th Biennial SGA Meeting,* Townsville, Australia, pp. 589–591.

Everhart DL (1985) Tectonic settings of the world's sandstone-type uranium deposits. In: Finch WI and Davis JF (eds.) *Geological Environments of Sandstone-Type Uranium Deposits: Report of the Working Group on Uranium Geology Organized by the International Atomic Energy Agency, IAEA-TECDOC-328*, pp. 21–46. Vienna: International Atomic Energy Agency.

Farges F, Ponader CW, Calas G, and Brown GEJ (1992) Structural environments of incompatible elements in silicate glass/melt systems: II. U^{IV}, U^{V}, and U^{VI}. *Geochimica et Cosmochimica Acta* 56: 4205–4220.

Fayek M and Kyser TK (1997) Characterization of multiple fluid-flow events and rare-earth-element mobility associated with formation of unconformity-type uranium deposits in the Athabasca Basin, Saskatchewan. *The Canadian Mineralogist* 35: 627–658.

Finch WI and Davis JF (eds.) (1985) *Geological Environments of Sandstone-Type Uranium Deposits: Report of the Working Group on Uranium Geology Organized by the International Atomic Energy Agency, IAEA-TECDOC-328*. Vienna: International Atomic Energy Agency.

Finch R and Murakami T (1999) Systematics and paragenesis of uranium minerals. *Reviews in Mineralogy* 38: 91–179.

Freed RL and Peacor DR (1989) Variability in temperature of the smectite/illite reaction in Gulf Coast sediments. *Clay Minerals* 24: 170–180.

Frimmel HE and Minter WEL (2002) Recent developments concerning the geological history and genesis of the Witwatersrand gold deposits, South Africa. In: Goldfarb RJ and Nielsen RL (eds.) *Integrated Methods for Discovery: Global Exploration in the 21st Century, Society of Economic Geologists Special Publication 9*, pp. 17–45. Littleton, CO: Society of Economic Geologists, Inc.

Gandhi SS (2007) Significant unconformity-associated uranium deposits of the Athabasca Basin, Saskatchewan and Alberta, and selected related deposits of Canada and the world. *Geological Survey of Canada Open File 5005*; *Saskatchewan Industry and Resources Open File 2007–11*. Quebec: Geological Survey of Canada.

Gatzweiler R (1987) Uranium mineralization in the Proterozoic Otish Basin, central Quebec, Canada. In: Friedrich G, Gatzweiler R, and Vogt J (eds.) *Uranium Mineralization: New Aspects on Geology, Mineralogy, Geochemistry and Exploration Methods, Monograph Series on Mineral Deposits 27*, pp. 27–47. Berlin, Stuttgart: Gebrüder Borntraeger.

Gauthier-Lafaye F and Weber F (1989) The Francevillian (lower proterozoic) uranium ore deposits of Gabon. *Economic Geology* 84: 2267–2285.

Gauthier-Lafaye F, Weber F, and Ohmoto H (1989) Natural fission reactors of Oklo. *Economic Geology* 84: 2286–2295.

Györfi I, Hajnal Z, White DJ, et al. (2007) High-resolution seismic survey from the McArthur River region: Contributions to mapping the complex P2 uranium ore zone, Athabasca Basin, Saskatchewan. In: Jefferson CW and Delaney G (eds.) *EXTECH IV: Geology and Uranium EXploration TECHnology of the Proterozoic Athabasca Basin, Saskatchewan and Alberta*, *Geological Survey of Canada Bulletin* 588: pp. 397–412. Ottawa, ON: Geological Survey of Canada.

Hazen RM, Ewing RC, and Sverjensky DA (2009) Evolution of uranium and thorium minerals. *American Mineralogist* 94: 1293–1311.

Hazen RM, Papineau D, Bleeker W, et al. (2008) Review paper: Mineral evolution. *American Mineralogist* 94: 1693–1720.

Hecht L and Cuney M (2000) Hydrothermal alteration of monazite in the Precambrian crystalline basement of the Athabasca Basin (Saskatchewan, Canada): Implications for the formation of unconformity-related uranium deposits. *Mineralium Deposita* 35: 791–795.

Hiatt EE, Kyser TK, Fayek M, Polito P, Holk GJ, and Riciputi LR (2007) Early quartz cements and evolution of paleohydraulic properties of basal sandstones in three Paleoproterozoic continental basins: Evidence from in situ $\delta^{18}O$ analysis of quartz cements. *Chemical Geology* 238: 19–37.

Hoeve J and Quirt DH (1984) Mineralization and host rock alteration in relation to clay mineral diagenesis and evolution of the middle Proterozoic, Athabasca Basin, northern Saskatchewan, Canada. *SRC Technical Report* No. 187. Saskatoon, SK: Saskatchewan Research Council.

Hoeve J and Sibbald T (1978) On the genesis of Rabbit Lake and other unconformity-type uranium deposits in northern Saskatchewan, Canada. *Economic Geology* 73: 1450–1473.

Hoffman P (1988) United plates of America, the birth of a craton: Early Proterozoic assembly and growth of Laurentia. *Annual Review of Earth and Planetary Sciences* 16: 543–603.

Holk GJ, Kyser TK, Chipley D, Hiatt EE, and Marlatt J (2003) Mobile Pb-isotopes in Proterozoic sedimentary basins as guides for exploration of uranium deposits. *Journal of Geochemical Exploration* 80: 297–320.

IAEA (1985). Uranium deposits in volcanic rocks. *Proceedings of a Technical Meeting*, El Paso, TX, United States, 2–5 April 1984, 468 pp. Vienna: International Atomic Energy Agency.

IAEA (2009) *World Distribution of Uranium Deposits (UDEPO), with Uranium Deposit Classification, IAEA TECDOC 1629*. Vienna: International Atomic Energy Agency.

Jaireth S, McKay AD, and Lambert IB (2008) Sandstone uranium deposits associated with hydrocarbon-bearing basins: Implications for uranium exploration in Australia. *Australasian Institute of Mining and Metallurgy Publication Series* 5(2008): 25–26.

Janeczek J and Ewing RC (1992) Structural formula of uraninite. *Journal of Nuclear Materials* 190: 128–132.

Jefferson CW, Thomas DJ, Gandhi SS, et al. (2007) Unconformity-associated uranium deposits of the Athabasca Basin, Saskatchewan and Alberta. In: Jefferson CW and Delaney G (eds.) *EXTECH IV: Geology and Uranium EXploration TECHnology of the Proterozoic Athabasca Basin, Saskatchewan and Alberta, Geological Survey of Canada Bulletin* 588, pp. 23–68. Ottawa, ON: Geological Survey of Canada.

Kotzer TG and Kyser TK (1995) Petrogenesis of the Proterozoic Athabasca Basin, northern Saskatchewan, Canada, and its relation to diagenesis, hydrothermal uranium mineralization and paleohydrogeology. *Chemical Geology* 120: 45–89; 124: 283 (erratum).

Kröner A, Retief EA, Compston W, Jacob RE, and Burger AJ (1991) Single-grain and conventional zircon dating of remobilised basement gneisses in the central Damara Belt of Namibia. *South African Journal of Geology* 94: 379–387.

Kyser K and Cuney M (2009) Unconformity-related uranium deposits. In: Cuney M and Kyser K (eds.) *Recent and Not-So-Recent Developments in Uranium Deposits and Implications for Exploration*, *Mineralogical Association of Canada Short Course Series*, vol. 39, pp. 161–220. Quebec: Mineralogical Association of Canada.

Kyser TK, Hiatt E, Renac C, Durocher K, Holk G, and Deckart K (2000) Diagenetic fluids in Paleo-and Meso-Proterozoic sedimentary basins and their implications for long protracted fluid histories. In: Kyser TK (ed.) *Fluids and Basin Evolution,*

Mineralogical Association of Canada Short Course Series, vol. 28, pp. 225–262. Quebec: Mineralogical Association of Canada.

Lambert I, Jaireth S, McKay A, and Miezitis Y (2005) Why Australia has so much uranium. *AusGeo News* 80: 1–14.

Langmuir D (1978) Uranium solution-mineral equilibria at low temperatures with applications to sedimentary ore deposits. In: Kimberley MM (ed.) *Uranium Deposits: Their Mineralogy and Origin, Mineralogical Association of Canada Short Course Series*, vol. 3, pp. 17–55. Toronto, ON: University of Toronto Press.

Larsen LM and Sørensen H (1987) The Ilı´maussaq intrusion - Progressive crystallization and formation of layering in an agpaitic magma. In: Fitton JG and Upton BGJ (eds.) *Alkaline Igneous Rocks, Geological Society Special Publication* 30, pp. 473–488. London: Geological Society of London.

Lauri LS, Ramo OT, and Cuney M (2007) Source characteristics of U-enriched leucogranites of the Svecofennian orogen in southern Finland. In: Andrew CJ, et al. (ed.) *Digging Deeper: Proceedings of the 9th Biennial Meeting of the Society for Geology Applied to Mineral Deposits*, Dublin, Ireland, 20–23 August 2007, pp. 1165–1168. Dublin: Irish Association for Economic Geology.

Laverov NP, Velitchkin VI, and Shumilin MV (1992) Uranium deposits of the CIS: The main economic genetic types and their distribution. *Geologiya Rudnykh Mestorozhdeniy* 2: 3–18.

Law J and Phillips N (2006) Witwatersrand gold–pyrite–uraninite deposits do not support a reducing Archean atmosphere. In: Kesler SE and Ohmoto H (eds.) *Evolution of Early Earth's Atmosphere, Hydrosphere, and Biosphere – Constraints from Ore Deposits. GSA Memoirs* 198: pp. 121–141. Boulder, CO: Geological Society of America.

Lecheminant AN and Heaman LM (1989) Mackenzie igneous events, Canada: Middle Proterozoic hotspot magmatism associated with ocean opening. *Earth and Planetary Science Letters* 96: 38–48.

Leroy J and George-Aniel B (1992) Volcanism and uranium mineralisations: The concept of source rock and concentration mechanism. *Journal of Volcanology and Geothermal Research* 50: 247–272.

Li J-W, Zhou M-F, Li X-F, Li Z-J, and Fu Z-R (2002) Origin of a large breccia-vein system in the Sanerlin uranium deposit, southern China: A reinterpretation. *Mineralium Deposita* 37: 213–225.

Linnen RL and Cuney M (2005) Granite-related rare-element deposits and experimental constraints on Ta-Nb-W-Sn-Zr-Hf mineralization. In: Linnen RL and Samson IM (eds.) *Rare-Element Geochemistry and Mineral Deposits, Geological Association of Canada Short Course Notes*, vol.17, pp. 45–68. St. John's, NL: Geological Association of Canada.

Ludwig KR (1978) Uranium-daughter migration and U/Pb isotope apparent ages of uranium ores, Shirley Basin, Wyoming. *Economic Geology* 73: 29–49.

Ludwig KR (1979) Age of uranium mineralization in the Gas Hills and Crooks Gap districts, Wyoming, as indicated by U-Pb isotope apparent ages. *Economic Geology* 74: 1654–1668.

Ludwig KR and Simmons KR (1992) U-Pb dating of uranium deposits in collapse breccia pipes of the Grand Canyon region. *Economic Geology* 87: 1747–1765.

Ludwig KR, Simmons KR, and Webster JD (1984) U-Pb isotope systematics and apparent ages of uranium ores, Ambrosia Lake and Smith Lake districts, Grants mineral belt, New Mexico. *Economic Geology* 79: 322–337.

Manning DAC (1981) The effect of fluorine on liquidus phase relationships in the system Qz–Ab–Or with excess water at 1 kb. *Contributions to Mineralogy and Petrology* 76: 206–215.

Martin-Izard A, Arribas A, SR, Arias D, Ruiz J, and Fernandez FJ (2002) The Fe deposit, West-Central Spain: Tectonic-hydrothermal uranium mineralization associated with transpressional faulting of Alpine age. *The Canadian Mineralogist* 40: 1505–1520.

Mathieu R, Zetterstrom L, Cuney M, Gauthier-Lafaye F, and Hidaka H (2001) Alteration of monazite and zircon and lead migration as geochemical tracers of fluid paleocirculations around the Oklo–Okélobondo and Bangombé natural nuclear reaction zones (Franceville basin, Gabon). *Chemical Geology* 171: 147–171.

McGill BD, Marlatt JL, Matthews RB, Sopuck VJ, Homeniuk LA, and Hubregtse JJ (1993) The P2 North uranium deposit, Saskatchewan, Canada. *Exploration and Mining Geology* 2: 321–331.

McPhie J, Kamenetsky VS, Chambefort I, Ehrig K, and Green N (2011) Origin of the supergiant Olympic Dam Cu-U-Au-Ag deposit, South Australia: was a sedimentary basin involved? *Geology* 39: 795–798.

Mossman DJ (1999) Carbonaceous substances in mineral deposits: Implications for geochemical exploration. *Journal of Geochemical Exploration* 66: pp. 241–247

Mossman DJ, Goodarzi F, and Gentzis T (1993) Characterization of insoluble organic matter from the Lower Proterozoic Huronian Supergroup, Elliot Lake, Ontario. *Precambrian Research* 61: 279–293.

Neumann NL, Southgate PN, Gibson GM, and McIntyre A (2006) New SHRIMP geochronology for the Western Fold Belt of the Mt Isa Inlier: Developing a 1800–1650 Ma event framework. *Australian Journal of Earth Sciences* 53: 1023–1039.

Nex PAM, Kinnaird JA, and Oliver GJH (2001) Petrology, geochemistry and mineralization of post-collisional magmatism in the southern Central Zone, Damaran Orogen, Namibia. *Journal of African Earth Sciences* 33: 481–502.

OECD (2001) *Assessment of Uranium Deposit Types and Resources - A Worldwide Perspective. IAEA TECDOC 1258*. Vienna: International Atomic Energy Agency.

OECD/NEA-IAEA (2008) *Uranium 2007: Resources, Production and Demand (the Red Book)*. Paris: Organisation for Economic Co-operation and Development.

OECD/NEA-IAEA (2010) *Uranium 2009: Resources, Production and Demand (the Red Book)*. Paris: Organisation for Economic Co-operation and Development.

Oreskes N and Einaudi MT (1992) Origin of hydrothermal fluids at Olympic Dam; preliminary results from fluid inclusions and stable isotopes. *Economic Geology* 87: 64–90.

Oreskes N and Hitzman MW (1993) A model for the origin of olympic dam-type deposits. In: Kirkham RV, Sinclair WD, Thorpe RI, and Duke JM (eds.) *Mineral Deposit Modeling, Geological Association of Canada Special Paper* 40, pp. 615–633. St. John's, NL: Geological Association of Canada.

Otton JK (1984) Surficial uranium deposits in the United States of America; Surficial uranium deposits. In: *Surficial Uranium Deposits: Report of the Working Group on Uranium Geology Organized by the International Atomic Energy Agency, IAEA-TECDOC-322*, pp. 237–242. Vienna: International Atomic Energy Agency.

Pacala S and Socolow R (2004) Stabilization wedges: Solving the climate problem for the next 50 years with current technologies. *Science* 305: 968–972.

Page RW, Jackson MJ, and Krassay AA (2000) Constraining sequence stratigraphy in north Australian basins: SHRIMP U–Pb zircon geochronology between Mt Isa and McArthur River. *Australian Journal of Earth Sciences* 47: 431–459.

Parks GA and Pohl DC (1988) Hydrothermal solubility of uraninite. *Geochimica et Cosmochimica Acta* 52: 863–875.

Peiffert C, Cuney M, and Nguyen-Trung C (1994) Uranium in granitic magmas: Part 1. Experimental determination of uranium solubility and fluid-melt partition coefficients in the uranium oxide-haplogranite H_2O-Na_2CO_3 system at 720–770°C, 2 kbar. *Geochimica et Cosmochimica Acta* 58: 2495–2507.

Peiffert C, Nguyen-Trung C, and Cuney M (1996) Uranium in granitic magmas: Part 2. Experimental determination of uranium solubility and fluid-melt partition coefficients in the uranium oxide-haplogranite-H_2O-NaX (X=Cl, F) system at 770°C 2 kbar. *Geochimica et Cosmochimica Acta* 60: 1515–1529.

Polito PA, Kyser TK, Alexandre P, Hiatt EE, and Stanley CR (2011) Advances in understanding the Kombolgie Subgroup and unconformity-related uranium deposits in the Alligator Rivers Uranium Field and how to explore for them using lithogeochemical principles. *Australian Journal of Earth Sciences* 58: 453–474.

Polito PA, Kyser TK, Marlatt J, Alexandre P, Bajwah Z, and Drever G (2004) Significance of alteration assemblages for the origin and evolution of the Proterozoic Nabarlek unconformity-related uranium deposit, Northern Territory, Australia. *Economic Geology* 99: 113–139.

Polito PA, Kyser TK, Rheinberger G, and Southgate PN (2005a) A paragenetic and isotopic study of the Proterozoic Westmoreland uranium deposits, southern McArthur basin, Northern Territory, Australia. *Economic Geology* 100: 1243–1260.

Polito PA, Kyser TK, and Stanley C (2009) The Proterozoic, albitite-hosted, Valhalla uranium deposit, Queensland, Australia: A description of the alteration assemblage associated with uranium mineralisation in diamond drill hole V39. *Mineralium Deposita* 44: 11–40.

Polito PA, Kyser TK, Thomas D, Marlatt J, and Drever G (2005b) Re-evaluation of the petrogenesis of the Proterozoic Jabiluka unconformity-related uranium deposit, Northern Territory, Australia. *Mineralium Deposita* 40: 257–288.

Rainbird RH, Stern RA, Rayner N, and Jefferson CW (2007) Age, provenance, and regional correlation of the Athabasca Group, Saskatchewan and Alberta, constrained by igneous and detrital zircon geochronology. In: Jefferson CW and Delaney G (eds.) *EXTECH IV: Geology and Uranium EXploration TECHnology of the Proterozoic Athabasca Basin, Saskatchewan and Alberta, Geological Survey of Canada Bulletin* 588, pp. 193–210. Ottawa, ON: Geological Survey of Canada.

Robertson JA (1989). The Blind River (Elliot Lake) uranium deposits. *Uranium Resources and Geology of North America, IAEA-TECDOC-500*, pp. 111–147. Vienna: International Atomic Energy Agency.

Robinson AG and Spooner ETC (1984) Postdepositional modification of uraninite-bearing quartz-pebble conglomerates from the Quirke ore zone, Elliot Lake, Ontario. *Economic Geology* 79: 297–321.

Rogers JJW and Santosh M (2002) Configuration of Columbia, a Mesoproterozoic supercontinent. *Gondwana Research* 5: 5–22.

Romberger SB, De vivo B, Ippolito F, Capaldi G, and Simpson RR (1984) Transport and deposition of uranium in hydrothermal systems at temperatures up to 300 °C: Geological implications. In: De Vivo B, Ippolito F, Capaldi G, and Simpson PR

(eds.) *Uranium Geochemistry, Mineralogy, Geology, Exploration and Resources*, pp. 12–17. London: Institution of Mining and Metallurgy.

Rosenberg PE and Hooper RL (1982) Fission-track dating of sandstone-type uranium deposits. *Geology* 10: 481–485.

Ruzicka V, Eckstrand OR, Sinclair WD, and Thorpe RI (1995) Vein uranium. In: Eckstrand OR, Sinclair WD, and Thorpe RI (eds.) *Geology of Canadian Mineral Deposit Types, Geology of Canada Issue 8*, pp. 277–286. Ottawa, ON: Geological Survey of Canada.

Schaller T, Dingwell DB, Keppler H, Knoller W, Merwin L, and Sebald A (1992) Fluorine in silicate glasses: A multinuclear nuclear magnetic resonance study. *Geochimica et Cosmochimica Acta* 56: 701–707.

Shurilov AV, Polekhovskiy YS, Cuney M, and Kister P (2006) Age determinations of uranium mineralization of Ladoga area. In: *IGOD Conference 2006*, Russia.

Sibbald TII and Quirt D (1987) Uranium deposits of the Athabasca Basin. *Field Trip Guidebook: Trip 9. Saskatchewan Research Council Publication R-855-1-G-87*. Geological Association of Canada Annual Meeting, Saskatoon, 1987.

Theis NJ (1979) *Uranium-Bearing and Associated Minerals in Their Geochemical and Sedimentological Context, Elliot Lake, Ontario*. Geological Survey of Canada Bulletin 304. Ottawa, ON: Geological Survey of Canada.

Thomas DJ, Matthews RB, and Sopuck V (2000) Athabasca Basin (Canada) unconformity – Type uranium deposits: Exploration model, current mine developments and exploration directions. In: *Geology and Ore Deposits 2000: The Great Basin and Beyond: Symposium Proceedings*, Reno, Nevada, 15–18 May 2000, vol. 1, pp. 103–126. Reno, NV: Geological Society of Nevada.

Thompson TB (1988) Geology and uranium-thorium mineral deposits of the Bokan Mountain Granite Complex, southeastern Alaska. *Ore Geology Reviews* 3: 193–210.

Tremblay LP (1978) Geologic setting of the Beaverlodge-type of vein-uranium deposit and its comparison to that of the unconformity-type. In: Kimberley MM (ed.) *Uranium Deposits: Their Mineralogy and Origin, Mineralogical Association of Canada Short Course Series*, vol. 3, pp. 431–455. Toronto, ON: University of Toronto Press.

Turner-Peterson CE and Fishman NS (1986) Geologic synthesis and genetic models for uranium mineralization in the Morrison Formation, Grants Uranium Region, New Mexico. In: Turner-Peterson CE, Santos ES, and Fishman NS (eds.) *A Basin Analysis Case Study: The Morrison Formation, Grants Uranium Region, New Mexico, AAPG Studies in Geology* 22, pp. 357–388. Tulsa, OK: American Association of Petroleum Geologists.

Turpin L, Leroy J, and Sheppard SMF (1990) Isotopic systematics (O, H, C, Sr, Nd) of superimposed barren and U-bearing hydrothermal systems in a Hercynian granite, Massif Central, France. *Chemical Geology* 88: 85–96.

Vance R (2008) Uranium 2007; resources, production and demand. *International Geological Congress, Abstracts = Congres Geologique International, Resumes* 33

Velichkin VI, Kushnerenko VK, Tarasov NN, et al. (2005) Geology and formation conditions of the Karku unconformity-type deposit in the northern Ladoga region (Russia). *Geology of Ore Deposits* 47: 87–112.

Vielzeuf D and Holloway JR (1988) Experimental determination of the fluid-absent melting relations in the pelitic system: Consequences for crustal differentiation. *Contributions to Mineralogy and Petrology* 98: 257–276.

Wenrich KJ and Sutphin HB (1989) Lithotectonic setting necessary for formation of a uranium-rich, solution-collapse breccia-pipe province, Grand Canyon region, Arizona. *US Geological Survey Open-File Report 89–0173*. Denver, CO: US Geological Survey.

Wenrich KJ, Van Gosen BS, and Finch WI (1995) Solution-collapse breccia pipe U deposits. In: du Bray EA (ed.) *Preliminary Compilation of Descriptive Geoenvironmental Mineral Deposit Models, US Geological Survey Open-File Report 95–831*, pp. 244–251. Denver, CO: US Geological Survey.

Zhao G, Cawood PA, Wilde SA, and Sun M (2002) Review of global 2.1–1.8 Ga orogens: Implications for a pre-Rodinia supercontinent. *Earth-Science Reviews* 59: 125–162.

Zhou W, Liu S, Wu J, and Wang Z (2000) Sandstone type uranium deposits in NW China. In: *Uranium Production and Raw Materials for the Nuclear Fuel Cycle–Supply and Demand, Economics, the Environment and Energy Security, Proceedings of an International Symposium, Vienna, 20-24 June 2005. IAEA Proceedings Series IAEA-CN-128*, pp. 152–159. Vienna: International Atomic Energy Agency.